



OPEN ACCESS

EDITED BY

Munir Ahmad Nayak,
Indian Institute of Technology Indore, India

REVIEWED BY

Shiblu Sarker,
Virginia Department of Conservation and
Recreation, United States
Md Saquib Saharwardi,
King Abdullah University of Science and
Technology, Saudi Arabia

*CORRESPONDENCE

Latifa Ait Dhmane

✉ latifa.aitdhmane-etu@etu.univh2c.ma

RECEIVED 12 July 2024

ACCEPTED 13 November 2024

PUBLISHED 06 December 2024

CITATION

Ait Dhmane L, Saidi ME, Moustadraf J,
Rafik A and Hadri A (2024) Spatiotemporal
characterization and hydrological impact of
drought patterns in northwestern Morocco.
Front. Water 6:1463748.
doi: 10.3389/frwa.2024.1463748

COPYRIGHT

© 2024 Ait Dhmane, Saidi, Moustadraf, Rafik
and Hadri. This is an open-access article
distributed under the terms of the [Creative
Commons Attribution License \(CC BY\)](https://creativecommons.org/licenses/by/4.0/). The
use, distribution or reproduction in other
forums is permitted, provided the original
author(s) and the copyright owner(s) are
credited and that the original publication in
this journal is cited, in accordance with
accepted academic practice. No use,
distribution or reproduction is permitted
which does not comply with these terms.

Spatiotemporal characterization and hydrological impact of drought patterns in northwestern Morocco

Latifa Ait Dhmane^{1*}, Mohamed Elmehdi Saidi¹,
Jalal Moustadraf¹, Abdellatif Rafik^{2,3} and Abdessamad Hadri²

¹Geo-Resources, Geo-Environment and Civil Engineering Laboratory, Cadi Ayyad University, Marrakesh, Morocco, ²International Water Research Institute (IWRI), Mohammed VI Polytechnic University (UM6P), Benguerir, Morocco, ³National Center for Scientific Research/Institute of Combustion, Aerothermal Energy, Reactivity and Environment (ICARE), CNRS, Orleans, France

Drought assessment and management, intensified by global warming, present critical challenges in semi-arid Mediterranean regions, impacting environmental sustainability and economic stability. This study evaluates spatiotemporal drought risk in the Bouregreg watershed in northwest Morocco by integrating remote sensing data with various drought indices. The Standardized Precipitation Index (SPI), the Standardized Precipitation Evapotranspiration Index (SPEI), and the Standardized Temperature Index (STI) were utilized to assess meteorological drought over a 12-month period. The Temperature Conditions Index (TCI) was used to evaluate temperature-related conditions for agricultural drought, while the GRACE Drought Severity Index (GRACEDSI) assessed hydrological drought on a monthly scale. Additionally, trend analysis was performed using Mann-Kendall and Sen's slope methods, and Pearson correlations were conducted among the indices. The findings revealed an overall downward trend in drought indices, with evapotranspiration (SPEI) being the primary drought driver. Over the study period, there was a significant increase in total evaporation demand, largely attributed to rising temperatures (STI and TCI). Meanwhile, precipitation conditions (SPI) remained relatively stable, highlighting the impact of global warming on agricultural and hydrological drought severity patterns in recent years. The results further indicated that drought risk is more pronounced in the plateau and plain areas of the Bouregreg compared to the mountainous regions. In evaluating water reserves, total water storage (TWS) data obtained from the Gravity Recovery and Climate Experiment (GRACE) was utilized. Comparisons were made between *in situ* groundwater level (GWL) data and those from GRACE TWS at a resolution of 0.25°. Our results reveal concordant trends between the two datasets, despite the differences in resolution. The TWS appears to be strongly correlated with GWL measurements and precipitation data with a lag of 1–4 months. The findings underscored a significant decline in water reserves and worsening drought conditions in recent years. Correlation analyses also revealed a moderate relationship between this decline and the systematic temperature rise, suggesting shared trends influenced by other anthropogenic factors not accounted for in the analysis. In summary, these results underscore the vulnerability of the entire study area to various forms of drought, ranging from mild to extreme severity.

KEYWORDS

remote sensing, drought, GRACE/FO, TWS, GRACEDSI, SPI, SPEI, TCI

1 Introduction

Drought is a global environmental challenge due to its complexity and frequency, recognized as the most costly natural disaster worldwide, causing significant annual losses and affecting more people than any other natural disaster (Wilhite, 2000). It has substantial impacts on social life and economic development (Wang et al., 2021) and occurs when regional hydro-meteorological variables fall below normal levels (Tate and Gustard, 2000; Dai, 2010). In the context of climate change, drought poses significant challenges for water availability, affecting various sectors (Pokhrel et al., 2021). Droughts can be classified into several types: meteorological, hydrological, agricultural, and socio-economic (Mishra and Singh, 2010; Agha-Kouchak et al., 2015). While meteorological, hydrological, and agricultural droughts are defined by physical and climate-related variables, socio-economic drought is linked to water resource scarcity often caused by socio-economic factors (Amjath-Babu et al., 2019).

Globally, droughts are more severe and frequent in arid and semi-arid regions. For example, the Mediterranean region, which is highly vulnerable to climate change, has experienced a notable increase in hydrological and agricultural droughts, as documented in the sixth assessment report of the Intergovernmental Panel on Climate Change (IPCC, 2021) and recent studies (Lionello and Scarascia, 2018; Trambly et al., 2020; Cos et al., 2022). Understanding drought is crucial for effective river basin management, water resource conservation, soil protection, and maintaining aquatic ecosystems (Sarker, 2021; Abdi-Dehkordi et al., 2021; Penning et al., 2023). Knowledge of drought patterns is also essential for dam construction, reservoir planning, flood control, and hydropower generation (Gao et al., 2022; Singhal et al., 2023; Zhang and Shang, 2023).

In Morocco, water scarcity poses a major challenge, with surface and groundwater reserves at historically low levels. The country faces severe and recurrent droughts impacting various regions almost annually. Studies have analyzed rainfall trends, variability, and climate change impacts on water resources (El Alaoui El Fels et al., 2022; Saouabe et al., 2022; Boughdadi et al., 2023; Ouhamdouch et al., 2022), and evaluated drought characteristics using various indices (Fnguire et al., 2017; Hadri et al., 2021a,b, 2022; Hadria et al., 2019; Ouatiki et al., 2019; Elair et al., 2023; Hanadé Houmma et al., 2022). These indicators are vital for understanding and addressing drought-related issues. Remote sensing technology has advanced drought assessment by providing continuous data over time and space for various indicators, such as precipitation, temperatures, snow, evaporation, evapotranspiration, soil moisture, and total water storage (NASA, 2010; Wardlow et al., 2012; Krajewski et al., 2006). Satellite-based observations offer near-real-time global coverage, continuous data records, and enhanced spatial precision (Heumann, 2011; Barrett et al., 1990).

The Bouregreg watershed is one of the country's five major rivers and represents a typical example of the northwest region of Morocco. This watershed plays a crucial role in water supply for agriculture and the regulation of urban and natural ecosystems (Khattabi and Samira, 2006; Mahe et al., 2014). It provides drinking water to the two largest cities in the country: Rabat and Casablanca. Like the rest of Morocco, the Bouregreg is particularly vulnerable to drought and has experienced several drought episodes in the past and present (Ouharba et al., 2022, 2024; Mahdaoui et al., 2024). These droughts have had significant consequences, notably on ecosystems, agriculture,

and domestic water supply. The impacts of climate change on future droughts in the Bouregreg are therefore a major concern for stakeholders, including water managers and farmers.

Recent studies on the Bouregreg watershed in Morocco reveal significant impacts of climate change on drought and water resources. Mahdaoui et al. (2024) used climate and hydrological models to predict a reduction in river flows and an increase in droughts under various greenhouse gas emission scenarios, highlighting the need to adapt water management strategies. Ouharba et al. (2024) found that temperatures are expected to rise by 0.8 to 1.3°C by 2030, with a reduction in precipitation, which would exacerbate droughts and summer heatwaves, affecting water and agriculture. Brouziyne et al. (2020) noted that climate change would worsen droughts by increasing their frequency and intensity, reducing precipitation and river flows, posing major challenges for agriculture and water management systems. Finally, Elkharrim and Bahi (2014) used statistical downscaling to project future intensification of droughts, with significant implications for water resource management and agriculture in northwestern Morocco.

The present work is based on integrating potential evapotranspiration with precipitation as key variables for assessing drought severity (Reyniers et al., 2023). The Standardized Precipitation Index (SPI; McKee et al., 1993), widely used for its simplicity and exclusive reliance on precipitation data, is effective for drought monitoring and early warning. Improving upon the SPI, the Standardized Precipitation-Evapotranspiration Index (SPEI; Vicente-Serrano et al., 2010) uses the difference between precipitation and evapotranspiration, combining sensitivity to changes in water demand and the multi-temporal nature of the SPI. According to Vicente-Serrano et al. (2015), the SPEI shows significant and equal sensitivity to evapotranspiration and precipitation, as well as their climatic variations, compared to the Self-Calibrating Palmer Drought Severity Index (sc-PDSI; Wells et al., 2004) and the reconnaissance drought index (RDI) (Tsakiris and Vangelis, 2005).

Drought results from complex interactions between the atmosphere, hydrosphere, and human activities (Jiang and Zhou, 2021; Samaniego et al., 2018), primarily due to persistent precipitation deficits and high-temperature anomalies (Wu et al., 2022). Significant efforts have been made to gather information on these aspects (Hayes et al., 2011). Van Rooy (1965) and Xia et al. (2018) respectively proposed the Rainfall Anomaly Index (RAI) and the Temperature Anomaly Index (TAI), based on the abnormal deviations of precipitation and temperature from their corresponding contemporary historical values. Similar to TAI and RAI, state-based indices, such as the Temperature Condition Index (TCI) (Kogan, 1995), are also easy to construct and can effectively reveal the relative state of current water conditions (Zhang et al., 2022a). One crucial aspect of drought is the reduction in river flow and groundwater levels (Allen et al., 2011; Tigkas et al., 2012; El Mezouary et al., 2024). Measuring hydrological droughts requires *in situ* observations of hydrological variables, which are often limited (Chen et al., 2009; Shahid and Hazarika, 2010; Taylor et al., 2009). GRACE satellites, launched in March 2002, have been widely used to measure hydrological droughts, providing comprehensive assessments of surface and groundwater reserves (Zaitchik et al., 2008).

Although GRACE TWS gravitational data are estimated at a native resolution of approximately 120 km, they have an effective signal resolution of around 200,000 km² due to the spatial bandwidth limitations of GRACE/GRACE-FO (Tapley et al., 2019). It is therefore

recommended to limit the use of these data to time series analyses at the basin scale. In this study, however, we have explored the use of GRACE TWS data at a sub-grid resolution of 0.25°, in a purely exploratory framework. This approach aims to identify potential trends in groundwater level variations while acknowledging that this resolution exceeds the recommended limits for confirmative spatial interpretation.

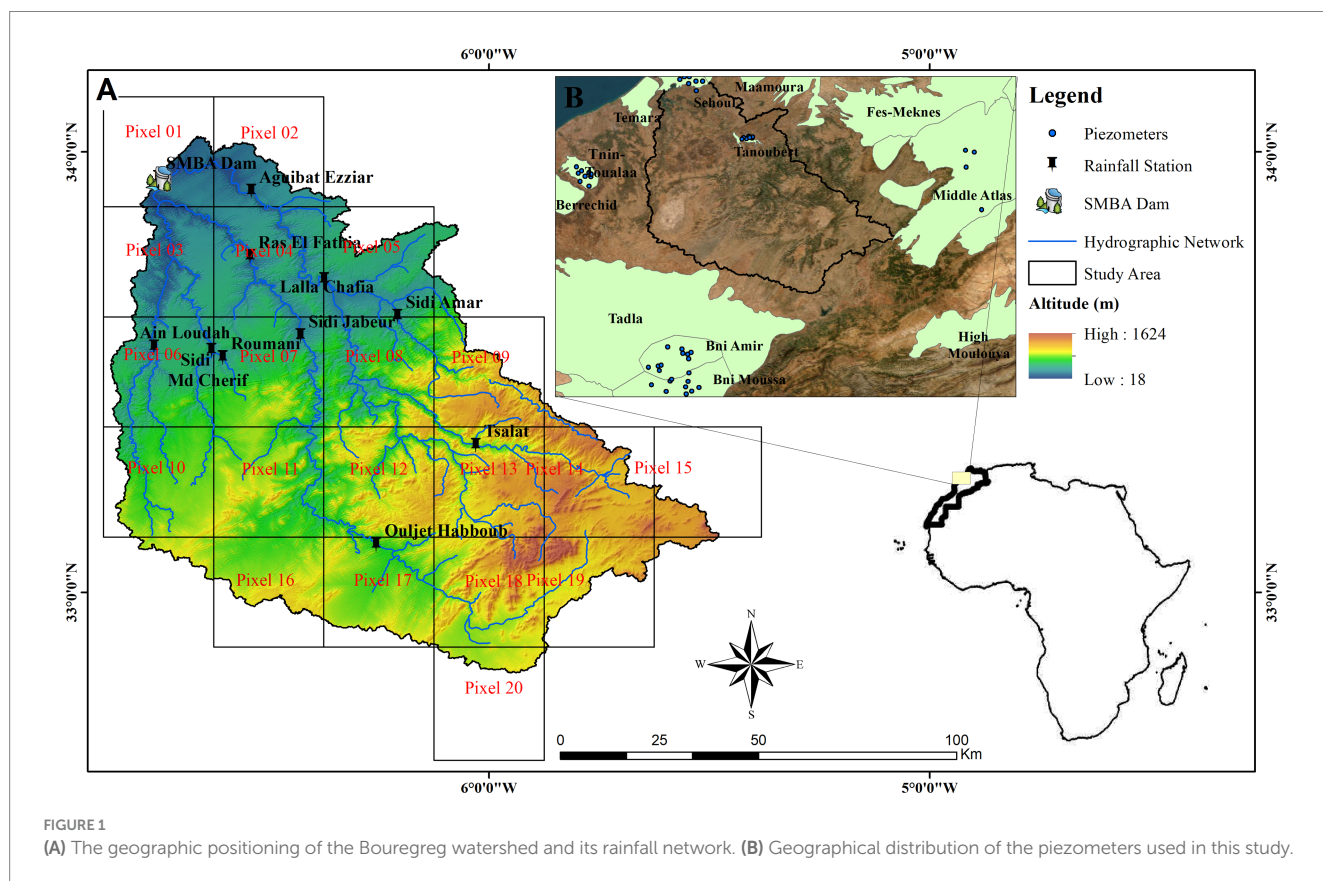
The aim of this paper is then to evaluate and enhance comprehension of drought risk and the ability to evaluate it by using various indices, including the Standardized Precipitation Index (SPI), the Standardized Precipitation-Evapotranspiration Index (SPEI), the Standardized Temperature Index (STI), the Temperature Condition Index (TCI) and the Drought Severity Index (DSI) based on data from the « Gravity Recovery and Climate Experiment » (GRACE) product. Furthermore, correlations between these indices will be established to assess their consistency and reliability. Finally, to evaluate the trends of these different drought indicators and their significance, we will employ the Mann-Kendall test (Kendall, 1975) temporally at 12-month scales and spatially at the scale of each pixel in the watershed. This is so that this study can provide information on the assessment and evolution of different types of drought in a semi-arid environment and in the context of climate change.

2 Methodology

2.1 Presentation of the study area

Located in the central-west of Morocco, the Bouregreg is a Mediterranean basin situated between latitudes 32.82 N and 34.04 N,

as well as longitudes 5.48 W and 6.86 W, spanning an area of 9,462 km² (Figure 1). Its boundaries are defined in the north and south by the recent Saiss and Ghareb trenches and the phosphate plateau, and in the east and west by the Middle Atlas mountains and the Atlantic Ocean, respectively. The Bouregreg, one of Morocco's main watercourses in terms of flow and size, is distinguished by its proximity, only 18 km from its mouth. It collects water from the center of Morocco, from the Middle Atlas to the Atlantic, which is retained by the Sidi Mohamed Ben Abdellah (SMBA) dam, constructed in 1974 with a storage capacity exceeding 1 billion m³, located near Rabat. Average annual rainfall in the area varies from 350 mm in the plain region to around 600 mm in the mountain region. The monthly average distribution of precipitation shows the existence of two identifiable seasons: (1) A rainy season, from October to April, during which the year's rainy episodes are concentrated, accounting for 86 to 92% of the annual rainfall; (2) A dry season, from May to September. Average temperatures in the region vary from 15 to 25°C in the mountains and from 30 to 34°C in the plain (HBABC, 2019). Evaporation is high throughout the Bouregreg basin. According to the Ministry of Energy, Mines, Water, and Environment, it is 1,600 mm/year in the Rabat-Salé coastal area and 800 mm/year in the upper Bouregreg. Evapotranspiration calculated according to Thornthwaite shows that the average annual deficit is everywhere greater than 250 mm, namely: 269 mm in the high plateaus, 435 mm in the low plateaus, 400 mm to 450 mm in the coastal zone (Tra Bi, 2013). Its hydrological climate is characterized by a notable decrease in precipitation since 1979, as well as an increase in extreme temperature events and heatwaves (El Aoula et al., 2021). This watershed is mainly devoted to rainfed cereal cultivation and is also



renowned for its pastures, being part of the favorable pastoral areas of the kingdom.

2.2 Data

Within the scope of this research, 10 rainfall stations were utilized to apply the pixel-to-point comparison between simulated and observed data from the Bouregreg watershed, aiming to assess meteorological drought in the Bouregreg watershed. These monitoring stations, operated by the Bouregreg and Chaouia Hydraulic Basin Agency (HBABC), recorded data on a daily basis spanning from January 1985 to August 2022 (Supplementary Table S1). Additionally, 56 piezometers from seven underground aquifers were used to evaluate and validate total water storage (TWS) data acquired from GRACE (Figure 1B). These piezometric data, provided by several hydraulic basin agencies, were used in the form of monthly chronological series (Table 1).

For spatiotemporal evaluation of meteorological drought in terms of precipitation, monthly data from the GPM-F satellite precipitation product were also employed. The Integrated Multi-satellite Retrievals for GPM (IMERG V06) product is developed by NASA in collaboration with the Japan Aerospace Exploration Agency (JAXA) and succeeds the Tropical Rainfall Measuring Mission (TRMM) satellite mission. It offers a high spatial and temporal resolution of 0.1° and 0.5 h. IMERG comprises three versions: Early Run (ER), Late Run (LR), and Final Run (FR), published, respectively, 4 h, 12 h, and 3.5 months subsequent to observations (Li et al., 2020). The first two versions are quasi-real-time products suitable for time-sensitive applications, whereas the FR version, used in this research, is calibrated using monthly Global Precipitation Climatology Centre (GPCC) data, providing more precise precipitation data (Chiaravalloti et al., 2018). In the Bouregreg watershed, studies assessing the performance of precipitation products conducted by Ait Dhmane et al. (2023), have proven that the GPM-F product is the most effective among four precipitation products examined at different scales.

ERA5 represents the fifth iteration of atmospheric reanalysis data provided by the ECMWF, covering a period extending from 1940. It succeeds the previous version, ERA-Interim, which only covered the period from 1979 and was established in 2006. ERA5 was built upon the Cy41r2 integrated forecasting system, which has been operational since 2016. It incorporates over a decade of advancements in model physics, core dynamics, and data assimilation (Hersbach et al., 2020). The ERA5 product refers to the high-resolution version of these data, characterized by a spatial and temporal resolution of 0.25° and 1 h. In this study, we used the ERA5 advanced dataset for 2m temperature (T2m) to assess meteorological drought in terms of air temperature and evapotranspiration, as well as the ERA5 dataset for land surface temperature (LST) to evaluate agricultural drought.

The Gravity Recovery and Climate Experiment (GRACE) and its follow-up mission, GRACE-FO are two similar initiatives conducted by NASA and the German Aerospace Center (DLR), launched in March 2002 and May 2018, respectively. Their main objective is to map monthly variations in Earth's gravity induced by the redistribution of mass on and beneath the Earth's surface. Three institutions, CSR (University of Texas/Center for Space Research), JPL (NASA Jet Propulsion Laboratory) and GFZ (Geo Forschungszentrum Potsdam), are responsible for processing GRACE data, providing data

on equivalent liquid water thickness in cm. Each institution is tasked with processing level 2 datasets (Landerer and Swenson, 2012; Banerjee and Kumar, 2018). Coefficients are generated independently by each center. Two main GRACE/FO data sets are available: spherical harmonic coefficients (SHC) and mass concentration solutions (mascons). Mascons are introduced as an alternative to address gravitational signals, offering advantages over spherical harmonics by being less prone to leakage errors and providing clearer distinction of land-ocean signals (Landerer and Cooley, 2021; Luthcke et al., 2013; Watkins et al., 2015). Total Water Storage (TWS) aggregates water masses present in various land reservoirs (Rodell and Famiglietti, 2001) (Equation 1). In this study, two variants of GRACE/FO mascon products, namely CSR and JPL's Mascon RL06.1V03 monthly data sets, featuring a spatial resolution of 0.25° , were used to generate Total Water Storage Anomaly (TWSA) in grid format. To explore how GRACE TWS data at this sub-grid resolution compares with *in situ* groundwater level observations, we analyzed whether the 0.25° scale data could reveal meaningful trends and correlations in groundwater variations at smaller scales. This approach is exploratory and does not imply that GRACE TWS data at a 0.25° resolution are suitable for confirmative spatial analysis.

$$TWS = SM + GWS + SWB + SW + Ca \quad (1)$$

With SWB, SWE, SM, GWS, and Ca representing, respectively, Surface Water Bodies, Snow Water Equivalent, Soil Moisture, Groundwater Storage, and Canopy. Some terms of the equation may be neglected depending on their impact on long-term variations of TWS (Shen et al., 2015).

2.3 Drought indices

Several indices are used to assess drought or humidity conditions in a specific region, covering various time scales. At the one-month scale, they reveal short-term conditions closely linked to meteorological droughts, providing crucial insights into soil moisture and crop stress, particularly throughout the growing season. The three-month scale offers a short to medium-term perspective, allowing estimation of seasonal precipitation and highlighting humidity conditions in key agricultural regions. Over six months, these indices identify seasonal precipitation trends, providing a detailed view of variations throughout different seasons. The nine-month scale provides an overview of interseasonal precipitation patterns, crucial for understanding drought development, often influencing agriculture and other sectors (Hao et al., 2015; Hayes et al., 2006; Mishra and Singh, 2010; Svoboda et al., 2012). Finally, at 12 months, these indices are often linked to reservoir levels, streamflow and even groundwater levels over longer periods. In this study, focused on the characterization and hydrological impact of drought, a 12 months scale was chosen (Figure 2).

The study area has a low density of hydroclimatic networks, with only 1,087 km² per station (HBABC, 2019). The upstream areas of the watershed require additional efforts due to insufficient coverage. The network is denser in the plains than in the high-altitude areas, contrary to the World Meteorological Organization (WMO) minimum recommendations. Additionally, the pixel-wise approach offers several advantages for drought evaluation, including high spatial

TABLE 1 Proprieties of the aquifers considered in this analysis.

| Aquifer's name | Index | Period | Number of piezometers | Thickness of the aquifer | Depth of the water table | Description |
|----------------|-------|-----------------|-----------------------|---------------------------|---|---|
| Tanoubert | 21 | 05/2008–11/2020 | 6 | 3–22 m | 4–16 m | It is a shallow unconfined aquifer flowing within alluvial deposits consisting of yellowish sands with interbedded conglomerate sandstones and bioclastic limestones overlying Triassic basalts and clays (HBABC, 2019). |
| Schoul | 13–14 | 05/2008–08/2020 | 9 | 5–30 m | 10–65 m | It is a free aquifer, developed in terrains consisting of consolidated sandy limestone and sand from the Pliocene. The gray marls of the Pliocene are impermeable and play a dual role: they form a barrier to the feeding of Paleozoic schists and constitute the substratum of the Pliocene aquifer (HBABC, 2019). |
| Tnin-Toulaa | 20 | 05/2008–08/2020 | 9 | 2–95 m | 5–61 m | It is a free aquifer, limited by the Al Maleh river in the west, Nfifikh river in the east, and outcrops of schistose and clayey substrates to the south and north. The series encountered near the Al Maleh river are as follows: (a) Superficial red silts from the recent Quaternary; (b) Dune sands, marls, and conglomerates from the ancient Quaternary and Pliocene; (c) Limestones and marls from the Cretaceous as well as limestones from the Infracenomanian. Drilling carried out in the study area showed they are pellicular; (d) Red clays and basalts from the Triassic; (e) Schists and quartzites from the Ordovician in the northwest of the study area and to the north near the Nfifikh river (GeoAtlas, 2009). |
| Bni Amir | 36 | 09/2007–06/2017 | 10 | 10–400 m | 0–69 | The aquifer system in the Tadla region is defined as a sequence of hydrogeological units, closely interconnected and of varying importance. From upstream to downstream, we find: the phreatic aquifer of the Miocene–Pliocene–Quaternary, the calcareous-sandy aquifer of the Eocene, the Senonian carbonate aquifer, and the Turonian carbonate aquifer (or locally of the Cenomanian–Turonian) (HBAOER, 2007). The Miocene–Pliocene–Quaternary aquifer comprises of two layers, the Beni-Amir layer and the Beni Moussa layer, set apart by Oum er Rbia river, which makes them hydraulically independent. The two layers flow within the heterogeneous fluvio-lacustrine series complex, including alternations of silts, marls, marly limestones, lacustrine limestones, and conglomerates (Knouz et al., 2016). |
| Bni Moussa | 36–37 | 09/2007–06/2017 | 10 | | | |
| Ifrane | 22 | 05/2002–06/2021 | 3 | Lias Aquifer: 10–300 m | (a) few meters to 50m; (b) between more than 100 m and less than 1 m. | The Middle Atlas Causes aquifer spans approximately 4,600 km ² , bordered to the north by the Fes Meknes basin and to the south by the Middle Atlas. It can be distinguished as follows: (a) The calcareous-dolomitic aquifer of the Lias covering about 4,600 km ² ; (b) The Quaternary basaltic aquifer subdivided by a watershed line into two sub-basins: Tigra (546 km ²) and Timahdite (435 km ²). |
| Boulmane | 30 | 09/2018–06/2021 | 1 | | | |

resolution (Xu et al., 2014), enhanced detection of localized conditions (Wang et al., 2018), improved accuracy, detailed impact analysis, better data integration, and improved early warning systems (Rembold et al., 2019). For these reasons, a pixel wise approach using remote sensing data has been chosen for a reliable and accurate assessment.

2.3.1 The standardized precipitation index (SPI)

The Standardized Precipitation Index (SPI), elaborated by McKee et al. (1993), is extensively utilized meteorological index for detecting, evaluating, and characterizing droughts intensity and frequency at various time scales. It relies on precipitation data from a specific site and measures the precipitation deficit and its effects on various aspects such as reservoir storage, groundwater, soil moisture, streamflow and snow cover (Tsakiris and Vangelis, 2004). The SPI utilizes cumulative precipitation sums over specific periods, known as accumulation intervals, to improve the time series cumulative probability distribution. Typically, precipitation sums are fitted with a gamma distribution (using the maximum likelihood method),

though alternative distributions could also be applicable. To facilitate SPI values comparison at different times, the gamma distribution quantiles are converted to standard normal variables (Equation 2). Consequently, negative SPI values show precipitation below the median, while positive values show precipitation above the median (Supplementary Table S2). Within this study, the SPI was calculated using accumulated precipitation sums on a monthly basis (Equation 3).

$$g(X) = \frac{1}{\beta^\alpha \Gamma(\alpha)} X^{\alpha-1} e^{-X/\beta} \tag{2}$$

Where $\Gamma(\alpha)$ is the Gamma function. α and β represent the shape and scale parameters, respectively.

$$SPI_{ijk} = \frac{P_{ijk} - \bar{P}_{ij}}{\sigma_{ij}} \tag{3}$$

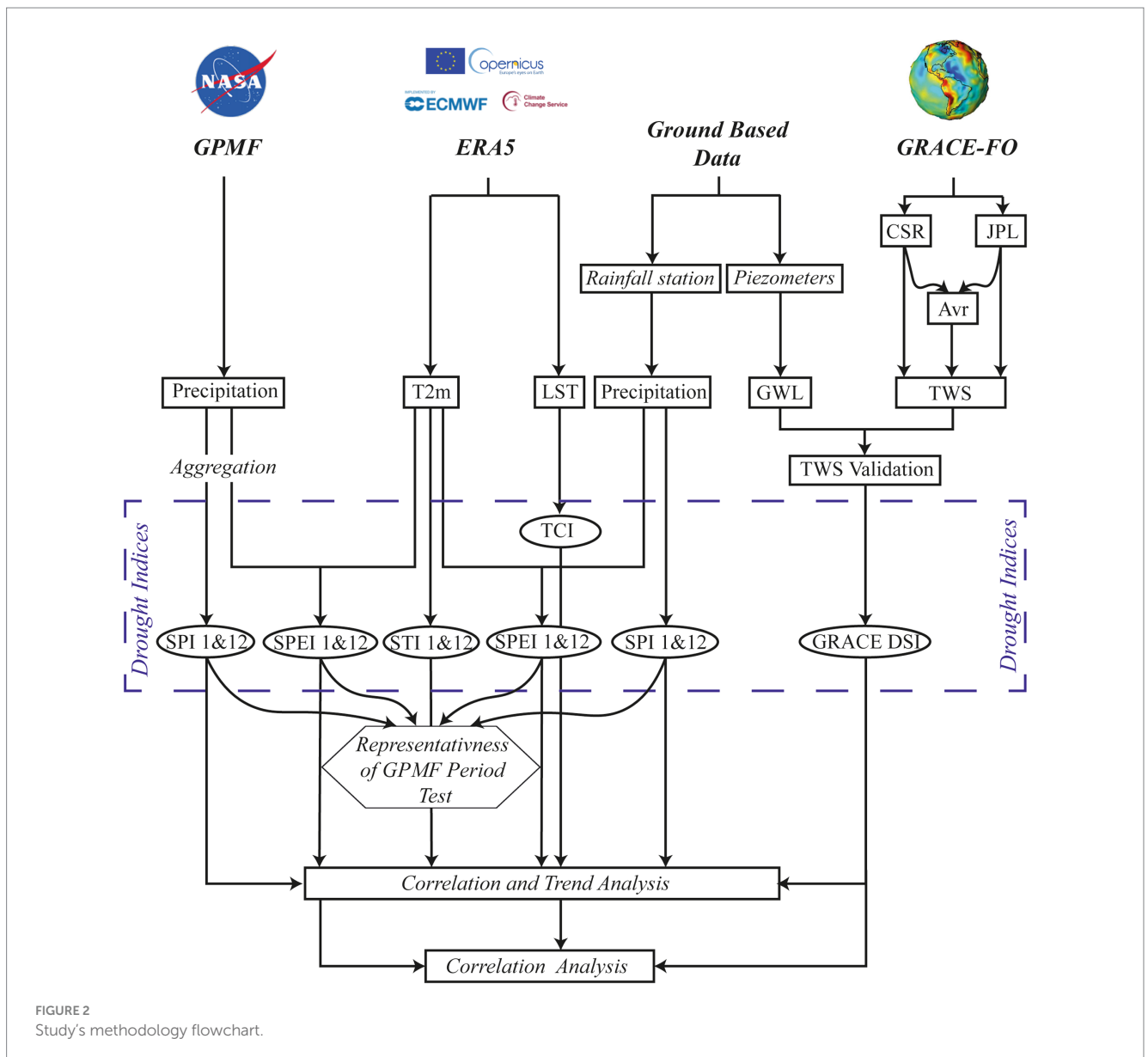


FIGURE 2 Study's methodology flowchart.

Where P_{ijk} represents the precipitation for pixel i during month j of year k , P_{ij} and σ_{ij} , respectively, denote the mean and standard deviation of precipitation for pixel i and month j over a period of n years.

2.3.2 The standardized precipitation evapotranspiration index (SPEI)

The Standardized Precipitation Evapotranspiration Index (SPEI) is a multi-scalar drought index (Vicente-Serrano et al., 2010; Beguería and Vicente-Serrano, 2009), derived from the monthly difference between precipitation and potential evapotranspiration (PET) (Equation 4), determined in this study by the Hargreaves-Samani method (HARG) (Hargreaves and Samani, 1985) (Equation 5). Er-Raki et al. (2010) evaluated the performance of three empirical methods in a similar context in Morocco for estimating reference evapotranspiration and found that the Hargreaves method is the most effective for estimating ET0, offering a viable alternative for PET estimation in semi-arid regions. Unlike other approaches that utilize various climatic parameters, such as the Penman-Monteith method endorsed by the FAO (Allen et al., 1998; Doorenbos and Pruitt, 1977; Monteith, 1965; Penman, 1948), the Hargreaves-Samani method relies solely on air temperature (Saharwardi et al., 2022). For this study, air temperature data utilized in the Hargreaves equation are sourced from ERA5 data. Estimating the SPEI requires a three-parameter distribution, unlike the SPI, which can be calculated using a two-parameter distribution like the gamma distribution (Vicente-Serrano et al., 2010). To obtain SPEI values for a specific period, a log-logistic distribution is fitted (Equation 6). Additionally, the SPEI uses the same drought categories as the SPI (Supplementary Table S2).

$$D_{ijk} = P_{ijk} - PET_{ijk} \quad (4)$$

Where D_{ijk} , P_{ijk} , and PET_{ijk} denote the deficit, precipitations, and potential evapotranspiration for pixel i during month j of year k .

$$PET = 0.408 a (T_a + 17.8)(T_{\max} - T_{\min})^{0.5} R_a \quad (5)$$

Where PET is expressed in [mm/day]; R_a is the extra-terrestrial radiation [MJ/m²/day]; T_a represents the average air temperature at 2 m height [°C]; T_{\max} and T_{\min} are the maximum and minimum air temperatures, respectively; the parameter 'a' in Equation 5 is an empirical constant, originally valued at 0.0023.

$$f(X) = \frac{\beta}{\alpha} \left(\frac{X - \gamma}{\alpha} \right)^{\beta-1} \left[1 + \left(\frac{X - \gamma}{\alpha} \right)^{\beta} \right]^{-2} \quad (6)$$

Where α , β and γ represent the scale, shape and origin parameters, respectively.

2.3.3 The standardized temperature index (STI)

STI is an index that quantifies the likelihood of a temperature value occurring relative to temperature values during a long-term period (Li et al., 2021; Darabi et al., 2023). It is calculated similarly to SPI, but unlike SPI, it does not accumulate temperature over a fixed scale (Equation 7). Assuming temperature variations follow a normal distribution, monthly temperature data has been modeled accordingly (Hansen et al., 2012; Zscheischler et al., 2014) (Equation 8). Positive

and negative values of STI indicate temperatures that are, respectively, higher and lower than the median temperature of the long-term period (Feng et al., 2021). It can be used to identify abnormally warm and cold periods (Supplementary Table S2).

$$STI_{ijk} = \frac{T_{ijk} - \bar{T}_{ij}}{\sigma_{ij}} \quad (7)$$

Where T_{ijk} represents the temperature at pixel i during month j of year k , P_{ij} and σ_{ij} , respectively, denote the mean and standard deviation of temperature for pixel i during month j over a period of n years.

$$f(X) = \frac{1}{\sigma\sqrt{2\pi}} e^{-\frac{1}{2}\left(\frac{X-\mu}{\sigma}\right)^2} \quad (8)$$

Where μ and σ^2 represent the mean and variance parameters, respectively.

2.3.4 Temperature condition index (TCI)

The TCI is utilized to assess vegetation stress resulting from high temperatures and humidity (Equation 9). Conditions are assessed based on maximum and minimum temperatures and adjusted to account for varying vegetation responses to temperature (Elair et al., 2023; Sun et al., 2008; Zhou et al., 2019). Generally, it is used together with NDVI and the Vegetation Condition Index (VCI, Kogan, 2000) to assess vegetation drought, especially when agricultural impacts are the primary focus. The temperature condition index considers that drought events reduce soil moisture, leading to thermal stress on land surfaces. During drought years, land surface temperatures (LSTs) are higher compared to the same month in normal years (Ghaleb et al., 2015). Elevated land surface temperatures during the season of crop growing suggest unfavorable or drought conditions, whereas lower temperatures indicate more favorable conditions (Singh et al., 2003; Bento et al., 2018) (Supplementary Table S3).

$$TCI = \frac{(LST_{\max} - LST)}{(LST_{\max} - LST_{\min})} \quad (9)$$

Where LST represent the value for a particular month and pixel, with LST_{\min} and LST_{\max} denoting the minimum and maximum values, respectively, for the same month and pixel throughout the climatological study period.

2.3.5 Impact of drought on groundwater resources

2.3.5.1 Validation of grace TWS data

In this section, the objective is to compare and validate GRACE Terrestrial Water Storage (TWS) data by comparing them with available piezometric data. Fifty-six piezometers from seven groundwater aquifers were used for this validation (Figure 1B). The Pearson correlation coefficient (Equation 10) was utilized to assess the linear relationship between GRACE and groundwater levels (GWL). Concordance with precipitation data and groundwater levels was also examined to determine the extent to which GRACE TWS data follow the temporal trends of GWL and precipitation observations. Piezometric data were inverted by multiplication by -1 to consider

that water levels are measured from the surface. All variables considered in this analysis were standardized (Figure 2).

$$\text{Power Corr} = \frac{\sum_{i=1}^N (X_i - \bar{X})(Y_i - \bar{Y})}{\sqrt{\sum_{i=1}^N (X_i - \bar{X})^2} \sqrt{\sum_{i=1}^N (Y_i - \bar{Y})^2}} \quad (10)$$

With X_i : the observation of GWL; Y_i : the observation of satellite TWS; \bar{X} : the average observation of GWL; \bar{Y} : the observation of satellite TWS; N : the sample size.

2.3.5.2 GRACE drought severity index (GRACEDSI)

GRACEDSI is a satellite-based drought index obtained from time-variable changes in terrestrial water storage (TWS) observed by satellite. It allows for comparison of drought characteristics between different regions and periods, while ignoring uncertainties associated with soil water balance models as well as the impact of meteorological data. Additionally, it takes into account changes in water storage resulting from human activities, such as groundwater extraction (Zhao et al., 2017a). In this study we emphasize on the exploratory nature of using 0.25° resolution GRACE data to observe groundwater trends. GRACEDSI is a dimensionless quantity that detects both drought and anomalously wet events (Supplementary Table S4). The calculation of GRACEDSI is as follows (Equation 11):

$$\text{GRACEDSI}_{i,j} = \frac{\text{TWS}_{i,j} - \overline{\text{TWS}}_j}{\sigma_j} \quad (11)$$

Where i represents the years from 2002 to the present, j represents the months from January to December, $\overline{\text{TWS}}_j$ and σ_j are the mean and standard deviation of TWS anomalies in month j , respectively.

2.4 Man Kendall's test

Within this study, an analysis was carried out on the spatiotemporal value of several drought indices, including SPI, SPEI, SRI, STI, TCI, and GRACEDSI. Additionally, the trend of each indicator was investigated by employing the Mann-Kendall test for each grid cell. The Mann-Kendall test is a non-parametric technique frequently employed in hydrological and climatological data analysis. Endorsed by the World Meteorological Organization (WMO), this approach is appreciated for its capacity to manage missing data and its robustness against outliers (Jamro et al., 2020). The MK test is applied to detect significant trends, either upward or downward, in hydrometeorological time series. In this study, the test results were derived using a significance level of 5% and a 95% confidence interval (Yue and Pilon, 2004). The trend statistic MK, Z_c is expressed as (Equations 12–16):

$$Z_c = \begin{cases} \frac{S-1}{\sqrt{\text{Var}(S)}}, & S > 0 \\ 0, & S = 0 \\ \frac{S+1}{\sqrt{\text{Var}(S)}}, & S < 0 \end{cases} \quad (12)$$

Where:

$$S = \sum_{i=1}^{n-1} \sum_{k=i+1}^n \text{sgn}(x_k - x_i) \quad (13)$$

$$\text{sgn}(x_k - x_i) = \begin{cases} 1, & x_k - x_i > 0 \\ 0, & x_k - x_i = 0 \\ -1, & x_k - x_i < 0 \end{cases} \quad (14)$$

$$\text{Var}(S) = \frac{n(n-1)(2n+5)}{18} \quad (15)$$

Where x_k and x_i represent the sequential data value, and n is the data length. The trend index, which measures the inclination, is expressed as follows:

$$\beta = \text{Median}\left(\frac{x_i - x_j}{i - j}\right) \quad (16)$$

Where: $1 < j < i < n$. A positive and negative β denotes a rising and decreasing trend.

3 Results and discussion

3.1 Characterization of meteorological drought

3.1.1 Pixel to point comparison

Due to the 23-year period of GPMF data, which is shorter than the period recommended by the World Meteorological Organization (WMO), this study uses data from ten rain gauge stations for a pixel-to-point evaluation. The objective is to test the representativeness of the 23-year period of GPMF data and to verify if they can be used for drought analysis with confidence, despite their shorter duration compared to the 30 years recommended by the WMO. It is therefore necessary to spatially match the index results for the station point measurements and the gridded estimates. To this end, the correlation between the drought indices SPI and SPEI calculated from GPMF data (23-year period) and those calculated from rain gauge station data (37-year period) was calculated (Figure 2 and Supplementary Table S1).

The correlation results show high values, ranging from 0.84 to 0.92 for SPI12 and from 0.82 to 0.95 for SPEI12 (Figure 3). These values indicate a strong positive relationship between the indices calculated from the two datasets and show that the two data series are strongly linked. These high correlations suggest that the 23-year period of GPMF data is representative of the longer 37-year period of rain gauge station data. This also means that the trends and variations of meteorological drought captured by the 23-year GPMF data are consistent with those observed over the 37-year period of the rain gauge stations. These high correlation values also indicate that satellite products, such as those from GPMF, are effective for characterizing meteorological drought in the investigation site and can be used with confidence to monitor and analyze drought.

3.1.2 By SPI and SPEI

The examination of the temporal and spatial evolution of precipitation revealed a large variability from year to year, with an average annual decrease in precipitation of -4.03 mm/year (ranging from -6.7 to -1.07 mm/year), although this decrease was not statistically significant. The analysis of the annual spatial distribution of precipitation showed that it is mainly influenced by altitude and distance from the coast in the study area. Regarding temperature, significant general trends were observed. Indeed, the average temperature recorded an average annual increase of $+0.05^{\circ}\text{C}$ (ranging from 0.001 to $0.14^{\circ}\text{C}/\text{year}$). Observations of the spatiotemporal distribution of temperature indicate a strong influence of altitude on temperatures.

This study examined the SPI and SPEI results for each cell within the study area from 2000 to 2023 (Supplementary Table S1). The findings revealed an alternation of drought, humidity, and normal conditions between 2000 and 2013 across the study area, except for a specific cell (Pixel 01) where wet months were more frequent in terms of SPEI due to the influence of the oceanic climate, characterized by moderate temperatures throughout the year (Figure 4). Between 2003–2004 and 2009–2011, the area experienced wet periods marked by abundant precipitation and an increase in anomalies or extreme events compared to the historical average or norm, particularly from 2009 to 2011. From 2014 onwards, significant changes were observed with a marked increase in the severity, frequency and duration of dry periods, leading to a deficit accumulation (Lee et al., 2017), except for the year 2018, which was wet in most parts of the area. Notably, between 2020 and 2021, the area experienced the most severe dry period over the entire study period, with pronounced effects in the plains and plateau areas compared to the mountainous zones (Figure 4).

Overall, dry conditions (SPI & SPEI < -1.0) occurred slightly more frequently than wet conditions (SPI & SPEI > 1.0), representing 34% of the conditions, while normal conditions ($-1.0 < \text{SPI} < 1.0$) were the most recurrent in the study area before 2009. Between 2009 and 2012, normal and wet conditions predominated, with their occurrence percentage nearly equivalent. After 2014, normal conditions with a trend towards dryness predominated across much of the study area. There was a notable increase in the frequency of dry conditions (SPI & SPEI < -1.0), accounting for 28% compared to 8% for wet conditions (SPI & SPEI > 1.0).

Spatially, the wettest year in the plain and plateau was 2010, while in the mountainous area, it was 2018. Conversely, the driest year in the plain and plateau was 2020 and in the southwest, it was 2014. Periods of severe drought were observed in 2001, 2005, 2014, 2016–2017 and 2020–2021 throughout the study area, with more pronounced intensity in the plain and plateau compared to the mountainous area (Figures 4, 5).

Figure 5 depicts the spatial distribution of droughts in the study area from 2010 to 2023 in March and September for the SPEI, TCI, and GRACEDSI indices. This distribution was obtained using interpolation by the kriging method. The results show notable seasonal variations, with more pronounced drought periods in September compared to March. By comparing the results obtained from the pixel-based approach and the spatial distribution approach, it appears that the two methods are complementary. The pixel-based approach provides fine and precise resolution at the level of individual

data points, while the spatial distribution approach, enhanced by kriging, offers a coherent overview of regional trends and patterns.

It is essential to compare the SPEI with the SPI to evaluate the influence of potential evapotranspiration (PET). Generally, there is a strong similarity between the SPEI and the SPI, especially in winter when PET tends to be lower than precipitation. Minimal differences between the SPEI and the SPI are typically observed in February and March.

The trends of the SPEI indicate a significant overall decrease across most study areas (Figures 4, 6), whereas the SPI remains relatively stable, particularly in mountainous regions. This rise in PET is attributed to increasing temperatures (Figure 7), which disrupts the water balance in the atmosphere and surface waters. This underscores the importance of concurrently considering both indices to comprehensively assess drought conditions in a given region.

In general, drought in the studied area is primarily attributed to an increase in evapotranspiration, particularly after 2013. Before this year, the impact of evapotranspiration was less pronounced, while significant variations in precipitation were the main cause of drought periods. Similarly, Vicente-Serrano et al. (2022) conducted a robust study analyzing meteorological drought trends and the impact of climate warming on drought severity over the past four decades, highlighting a notable rise in atmospheric evaporation demand (AED) during this period.

3.1.3 By STI

This study investigated the STI index at 12-month for every cell within the Bouregreg watershed spanning from 1990 to 2023 (Supplementary Table S1). In general, the results of the Standardized Temperature Index (STI) show a significant general trend towards increasing temperatures (Stour and Agoumi, 2009; Khomsi et al., 2013; Woillez, 2019) and drought in the majority of the study area (Figures 6D–H, 7). STI analysis indicates that recent years have been hotter than previous years, particularly from 2010 onwards, except for the first cell where the oceanic climate influences the area and the last two cells, influenced by specific weather conditions associated with high-altitude areas and the topography of mountainous regions.

The results of the STI analysis show that hot periods began gradually from 1995, with an increase in dry period compared to the previous period, which was characterized by wet conditions throughout the study area. This trend towards drought intensified noticeably since 2010, with higher levels of drought than before.

Among the early years of the study (before 1995), only the year 1993 (15.7°C) was classified as extremely humid year, while the other years had an STI < -1 , indicating different categories of cold conditions. The percentage of warm or warm-trending periods significantly increased from 1995 to 2010, although there is generally an alternation of drought, humidity, and normal conditions, except for Pixel 15 where normal to cold-trending conditions persist until 2012. Surprisingly, for the last two cells (Figure 7), higher normal to warm-trending conditions were observed than in the rest of the study area.

After 2010, the frequency and intensity of drought increased compared to the previous period. STI values show a trend towards extreme drought in the plain and plateau areas. A sudden transition from normal to cold-trending conditions to warm conditions was observed in the cell (Pixel 15) in 2013. In contrast, normal to cold-trending conditions are observed for the last two cells (Figure 7). Overall, a decline in the frequency and intensity of wet years was

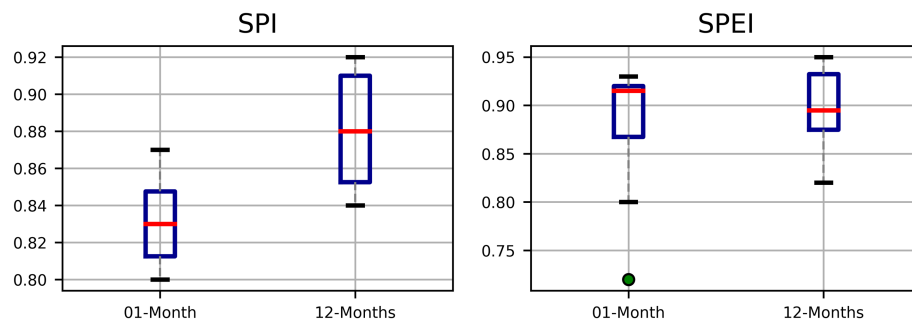


FIGURE 3 Correlation between SPI&SPEI from GPMF data and rain gauge data (Red line: Median).

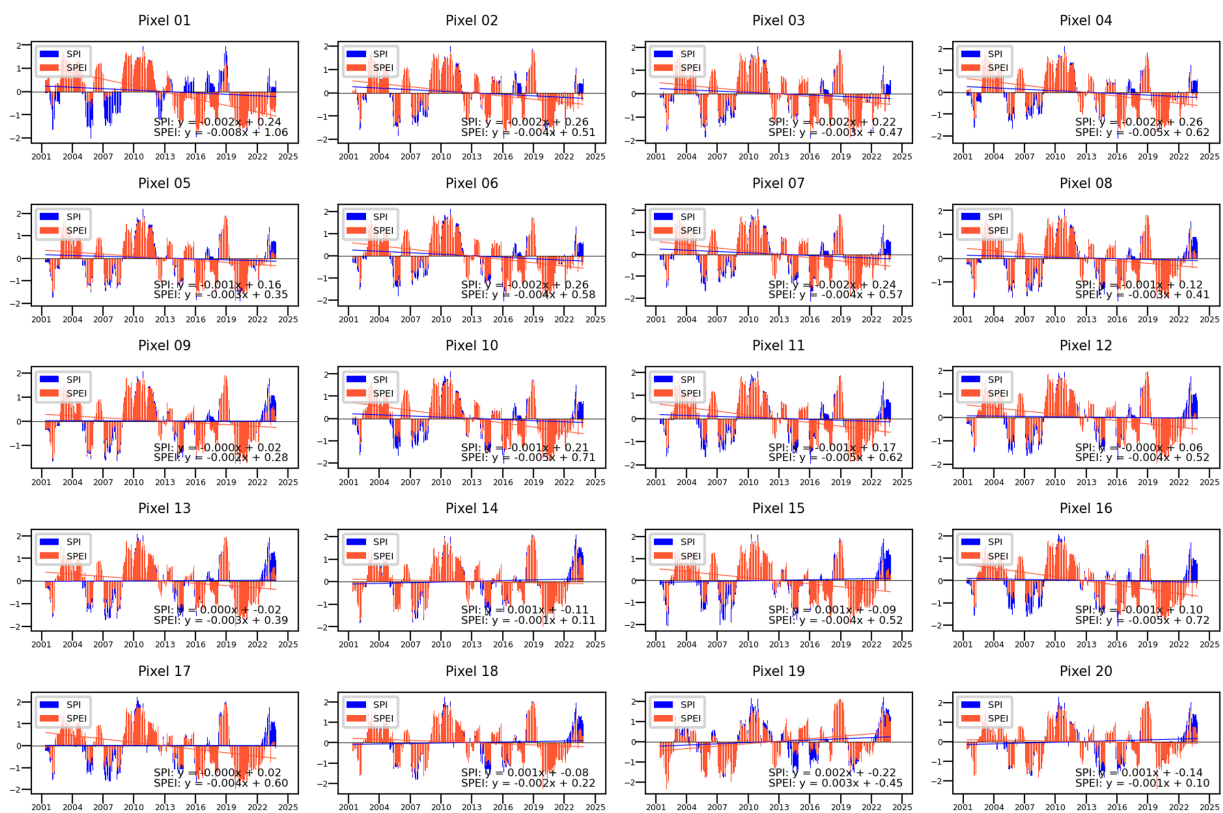


FIGURE 4 Drought's spatiotemporal evolution using the SPI12 and SPEI12 in the Bouregreg watershed.

noted for this period, indicating a significant decrease in normal to cold conditions over the years.

Overall, severe drought periods were observed in 1995 (17.6°C), 2001 (17.77°C), 2006 (17.6°C), 2010 (17.83°C), 2017 (18.63°C), and 2023 (19.54°C), with more pronounced intensity in the plain and plateau compared to the mountainous area. For the year 2010, although it was classified as humid in terms of SPI and SPEI, it was simultaneously warm in terms of STI. These indices evaluate different aspects of the climate and often exhibit independent variations from each other. Thus, a year may have abundant precipitation (high SPI and SPEI) while displaying high temperatures (high STI), which can result from various weather and climate conditions such as irregular

precipitation patterns or regional thermal anomalies. In conclusion, this combination of indices indicates an increased risk of drought due to higher temperatures and relatively stable precipitation conditions.

3.2 Characterization of drought by TCI

In this section, the use of TCI, based on LST data, to assess agricultural drought is justified by the strong correlation between soil temperatures and soil water availability (Holzman et al., 2021), especially during dry periods. High soil temperatures can have adverse effects on crops, notably by accelerating soil moisture evaporation and

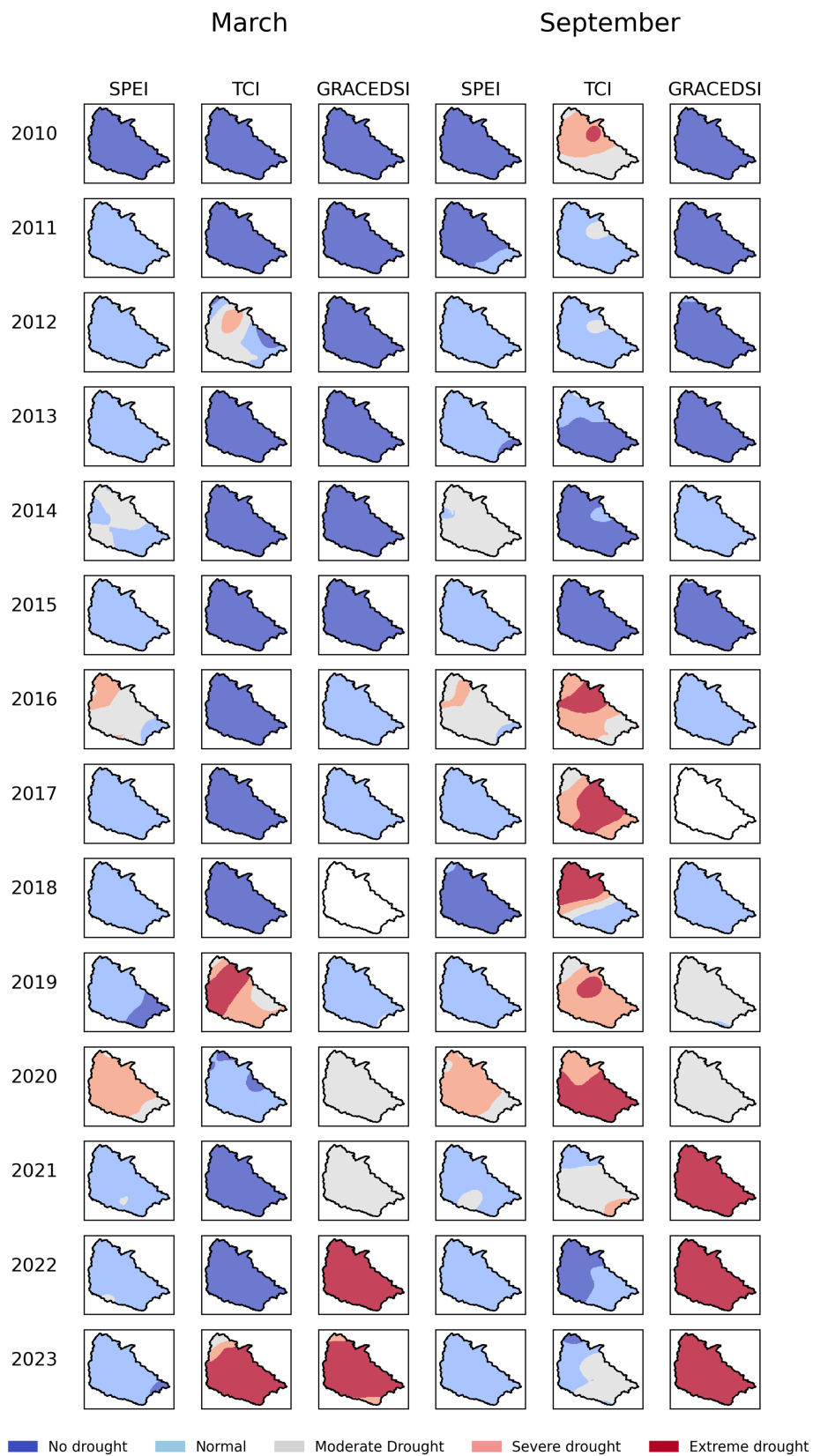
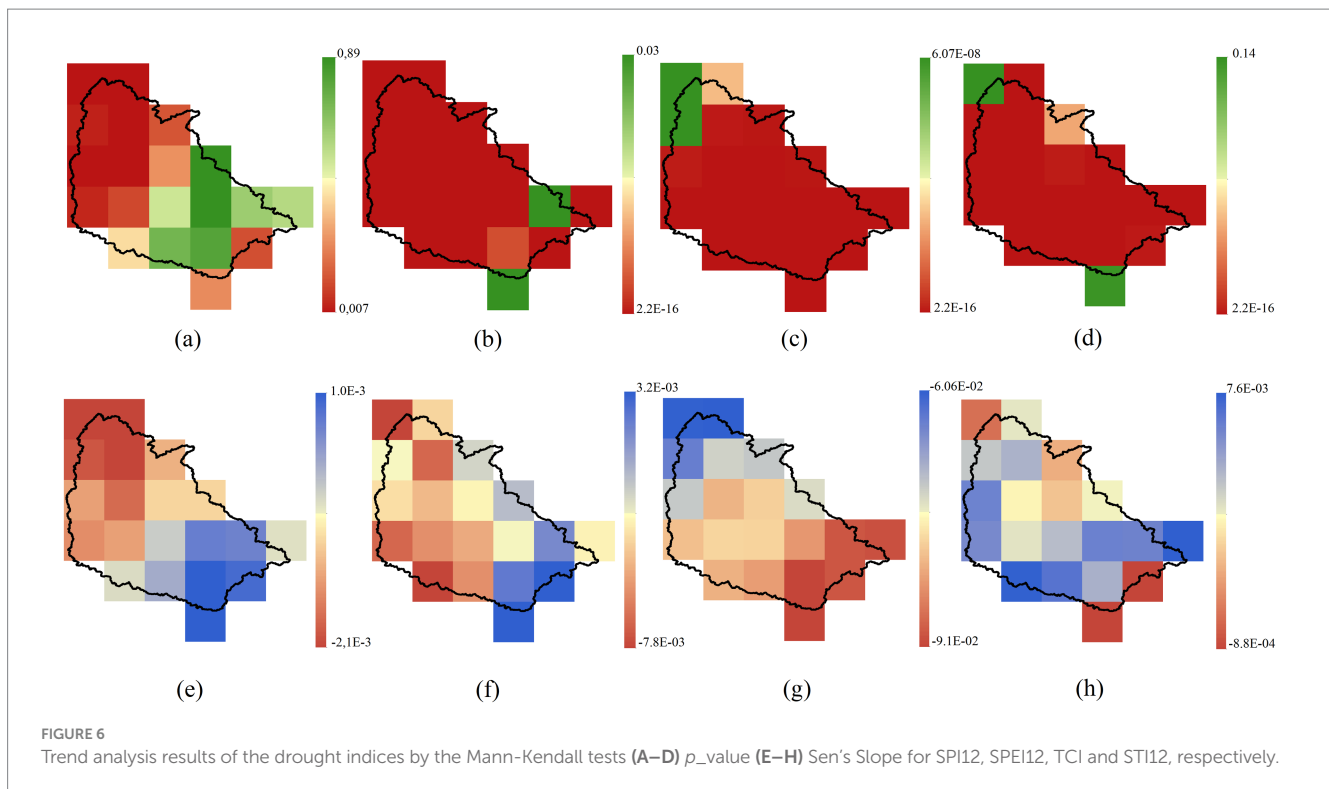


FIGURE 5
Drought's spatial patterns across the study area from 2010 to 2023 in March and September.



inducing stress in plants (Rasheed et al., 2022). By focusing on soil temperature trends, it becomes possible to directly assess the impact of drought on crops, without relying exclusively on vegetation indicators. This study analyzed the TCI of each cell within the study area for the period from 1990 to 2023 (Supplementary Table S1).

The TCI (Temperature Condition Index) is developed to consider vegetation response to temperature. Temperatures are evaluated based on extreme conditions. TCI data reveal an overall downward trend (Figures 6C,G), indicating a progressive deterioration of conditions for crop development over the years (Figures 5, 8). They also indicate that the effective temperature of the land surface in recent years has been higher than that of previous periods in most of the study area, accompanied by an increase in the frequency of months characterized by dry and intense conditions.

Indeed, the frequency of months characterized by extreme drought conditions ($TCI \leq 10$) increased from 0% in 2014 to 16.67% in 2022, equivalent to an average of two extremely dry months per year. Conversely, the frequency of months without drought ($40 < TCI \leq 100$) decreased by 83.5% between the period of 2000 to 2013, representing an average of 10 months per year, to 58.3% between 2012 and 2022, corresponding to an average of 7 months per year. In terms of TCI, drought periods were observed in 2017 and 2022 across the entire study area, with the most severe being in 2017 (Figures 5, 8). On the other hand, the wettest periods occurred from 1991 to 1993, in 1996, and in 2004 across the entire study area, with TCI levels surpassing 65%.

The TCI represents the deviation between the temperature of the month under study and the recorded extreme values. Thus, an excessively temperature in the middle of the vegetation growth season (TCI close to zero) indicates unfavorable conditions for crop development. Overall, the results of TCI suggest an increase in the risk of agricultural drought due to the rise in surface temperatures, in

response to changes in meteorological conditions, notably the increase in air temperatures (Figure 7).

3.3 Correlation analysis

Within this study, a correlation analysis was carried out to examine the linear spatial and temporal relationship between drought indices, using the Pearson correlation coefficient (Equation 10). This analysis, which encompasses the drought indices SPI, SPEI, STI, and TCI, aims to elucidate the links between these different indicators and to assess their ability to detect and quantify drought periods. By studying the correlations between these various indices, we can better understand the relationships between meteorological conditions (such as precipitation and temperatures) and vegetation responses, as well as their impact on drought.

Figure 9 presents the spatiotemporal results of the Pearson correlation. High positive correlations, ranging from 0.68 to 0.84, indicate a fairly strong relationship between SPI and SPEI. This observation indicates a notable consistency between the periods of precipitation deficit or excess identified by the SPI and the fluctuations in evapotranspiration considered by the SPEI, reinforced by the inclusion of precipitation variations in the SPEI. Thus, the high correlations between these two indices stem from this dual consideration in the calculation of the SPEI. In contrast, very weak correlations between SPI and STI, as well as between SPI and TCI, on the plateau and in the plain, suggest a practically non-existent relationship. These results suggest that temperature fluctuations measured by STI and land surface temperature evaluated by TCI are not significantly related to precipitation deficits or excesses measured by SPI in these regions. However, these correlations increase as we move towards

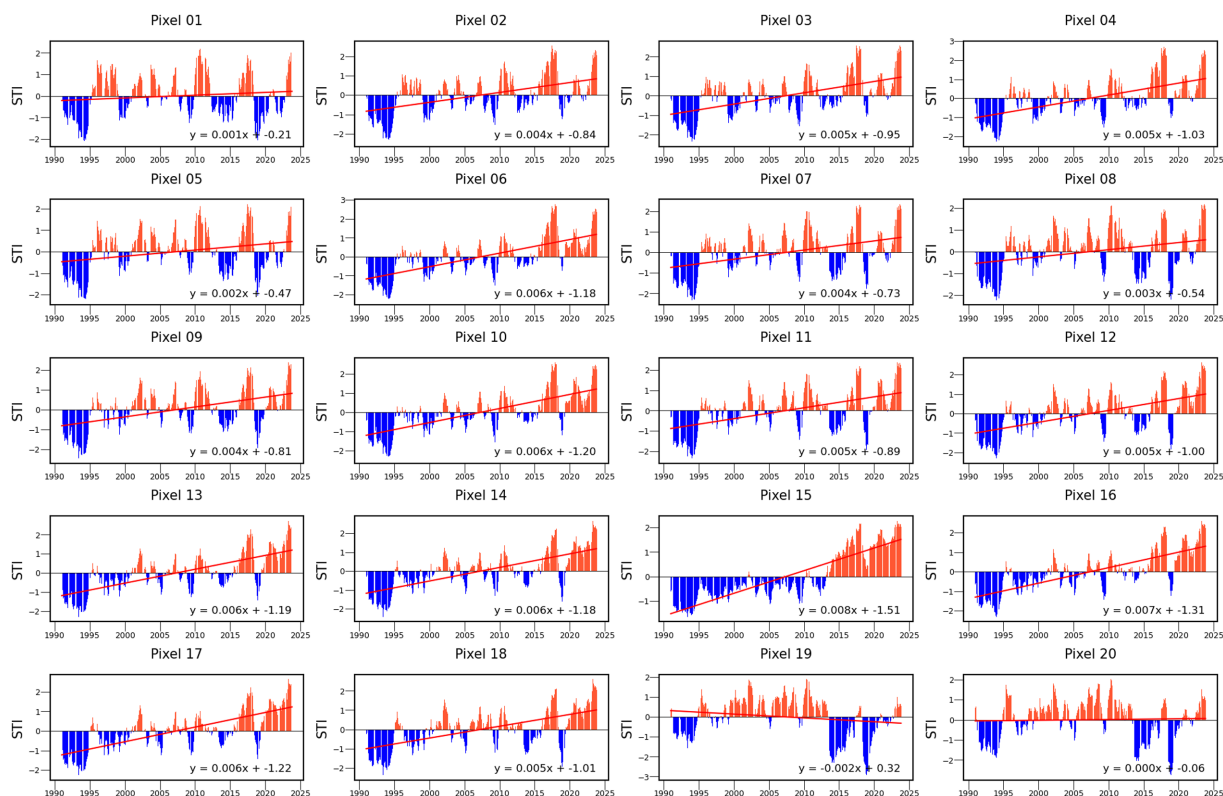


FIGURE 7
Drought's spatiotemporal evolution using the monthly STI12 in the Bouregreg watershed.

mountainous areas, indicating a slightly inverse relationship with temperature variations and a slight relationship with vegetation responses to temperature (Figure 9).

Regarding SPEI, negative correlations spanning from weak to moderate, from -0.25 to -0.56 , suggest a slightly inverse relationship between SPEI and STI. This suggests that the fluctuations in evapotranspiration considered in the SPEI are mildly to moderately linked to the variations in temperature assessed by the STI, especially on the plateau and in the plains, and moderately in mountainous areas. Furthermore, positive correlations ranging from moderate to high, from 0.34 to 0.6 , indicate a fairly strong relationship between SPEI and TCI. This finding suggests that temperature variations evaluated by TCI are in harmony with evapotranspiration fluctuations accounted for by SPEI (Figure 9).

Between STI and TCI, high negative correlations, ranging from -0.64 to -0.95 , indicate a very strong and inverse relationship between these two indices. This observation suggests that temperature variations evaluated by STI are closely associated with vegetation responses to temperature evaluated by TCI. Overall, these results suggest that SPEI and TCI are the most closely related indices, indicating a strong correlation between evapotranspiration variations and vegetation responses to temperature (Figure 9).

Indeed, the soil temperature is influenced by the air temperature with a time lag and variable amplitude depending on the depth, the type of vegetation present, as well as the terrain and subsurface variables. These thermal fluctuations, both at the surface and in depth, influence bioclimatic variations, water availability, and thus plant phenology (Rome et al., 2008).

Generally, the amplitude of soil temperature variation corresponds to that of air temperature but decreases exponentially with distance from the surface. Moreover, soil temperatures vary very little on average throughout the year at a depth of more than 5 to 6 m (Gold, 1967). Additionally, the maximum or minimum temperatures of deeper layers are reached with a time lag compared to the surface, with this delay increasing linearly with depth (Rome et al., 2008).

The LST plays an essential role in terrestrial surface processes, serving not merely as a marker of climate change but also as a regulator of the upward terrestrial radiation (Aires et al., 2001). The Earth's surface albedo, on the other hand, represents the proportion of radiation reflected compared to the incident radiation, and it is a crucial feature for managing the global radiative energy balance and radiative energy distribution between the atmosphere and the surface (Schaaf, 2009). While albedo measures the portion of reflected radiation, LST is associated with the quantity of radiation absorbed by the surface. These two combined elements influence the process of water transformation into vapor (Saher et al., 2021). The radiation absorption contributes to the increase in surface temperature, which can intensify evaporation demand (Rizwan et al., 2008; Schwarz et al., 2012; Taha, 1997). This phenomenon is particularly pronounced in arid regions, where vegetation is limited, resulting in an increase in sensible heat rather than latent heat (Templeton et al., 2018).

The strong negative correlations between STI and TCI indicate that as temperature fluctuations increase, temperatures at the soil surface also rise, altering the surface energy balance and resulting in a significant increase in atmospheric evaporation demand. In

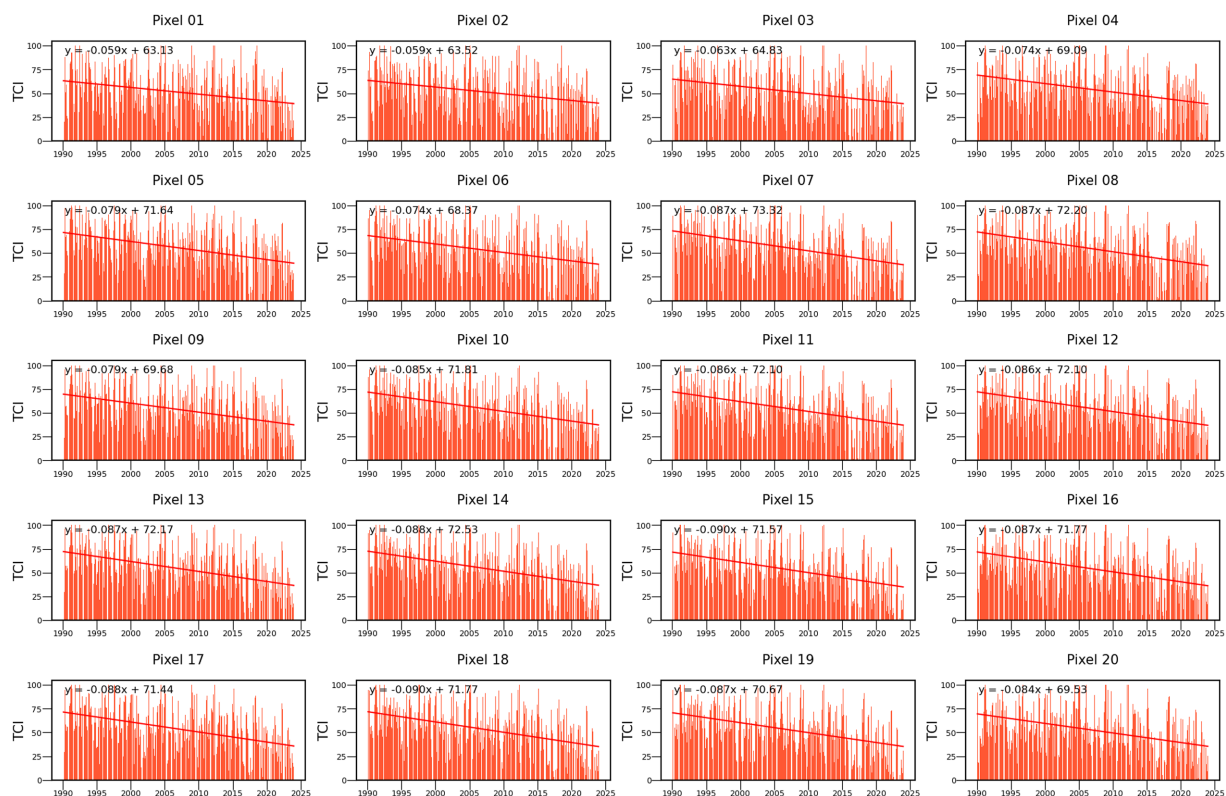


FIGURE 8
Drought's spatiotemporal evolution using the monthly TCI in the Bouregreg watershed.

agriculture, particularly for vegetated surfaces, ET can serve as an indicator of plant water stress (Jackson et al., 1981). This water stress, caused by water retention, affects both the physical environment of plant growth and the physiology of crops (Lisar et al., 2012; Kramer, 1980). Overall, the results indicating that SPEI and TCI are the most closely related indices underscore the importance of considering both water availability (represented by SPEI) and temperature (represented by TCI) in the assessment of meteorological and agricultural drought.

3.4 Characterization of hydrological drought

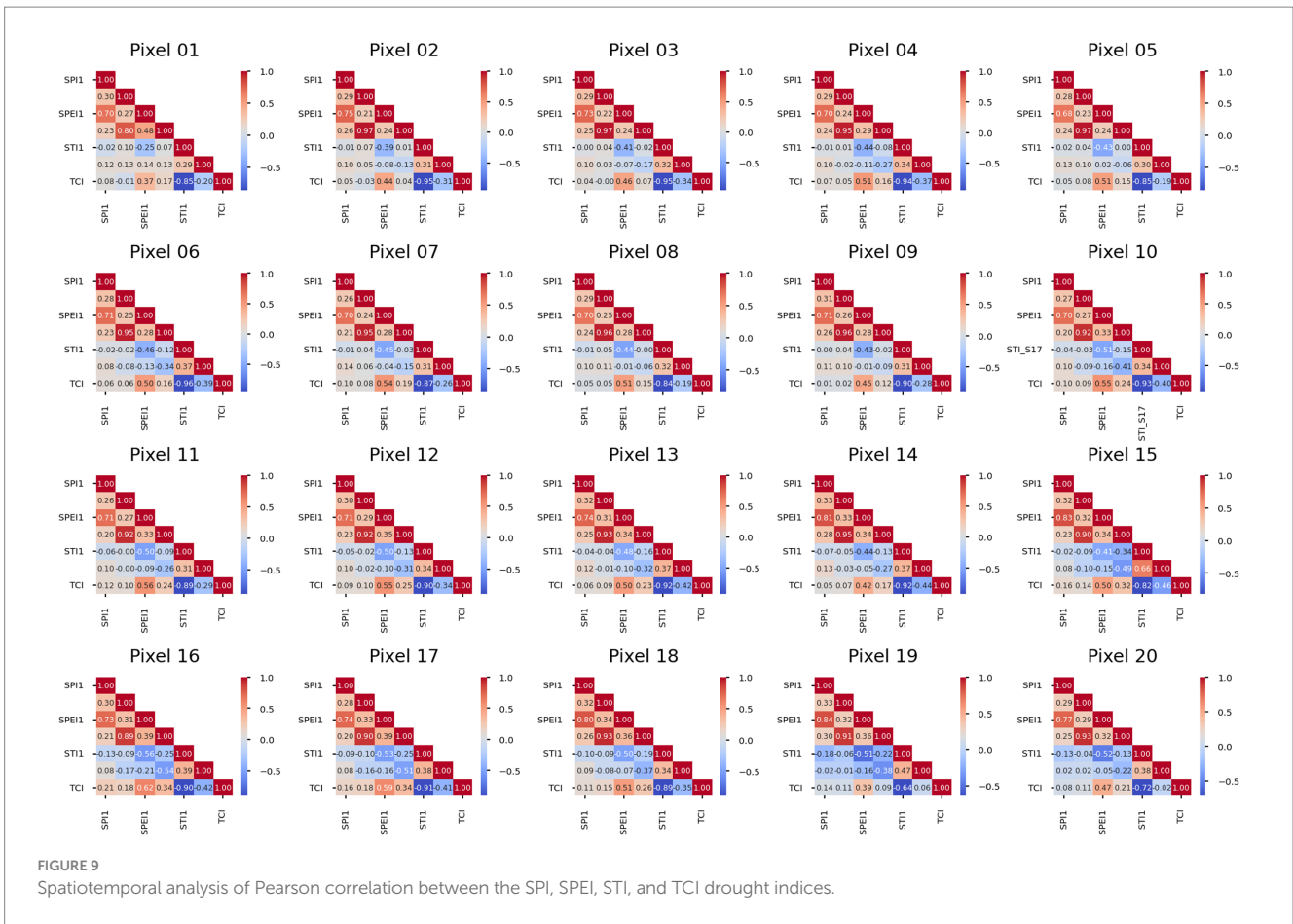
3.4.1 Validation of grace TWS data

The shortage of hydro-climatic data presents a notable challenge in various regions globally, with both qualitative and quantitative information on water resources, particularly groundwater levels (GWL), often being limited (Rafik et al., 2023a,b). In such cases, data on TWS can serve as a viable alternative for these regions. The objective of this section is to verify the validity of TWS data by comparing them with available piezometric data. The study's use of GRACE TWS data at a 0.25° resolution is experimental, as this resolution goes beyond the scale recommended by GRACE data providers. This exploratory approach seeks to determine if small-scale trends in GRACE data can capture local groundwater level variations, despite the resolution's limitations. In semi-arid and arid environment, groundwater often serves as the primary source of available water,

and its management is crucial for ensuring the sustainability of water resources. In these regions where aquifers are significant and precipitation may be limited, GWS can represent a significant portion of TWS.

The analysis concerning the correspondence between TWS data from GRACE, precipitation data, and groundwater levels was conducted to assess to what extent GRACE TWS data reflect the observed temporal trends of groundwater levels and precipitation. Figure 10 illustrate this agreement for each aquifer (Supplementary Figures S1–S6). Normalization of the data was implemented to facilitate comparison on a consistent scale. Overall, our results show good to very good agreement of TWS data (CSR, JPL, and Avr) with *in situ* observations and precipitation data. However, while the sub-grid scale analysis reveals high consistency with the observed groundwater trends, smaller discrepancies might be expected due to the inherent spatial limitations of GRACE data. This supports that GRACE TWS effectively captures regional trends, although precision may vary across specific areas and timeframes. Furthermore, the time series of TWS provided by CSR seems to better capture the temporal patterns of groundwater levels than that provided by JPL.

In this section, the Pearson correlation was also used to explore the linear relationship between piezometric data from 56 piezometers of seven groundwater aquifers and TWS. Additionally, a second correlation analysis was conducted between piezometric data and TWS after subtracting soil moisture (SM) data. The SM data used in this section were obtained from the Global Land Data Assimilation System coupled with the NOAA model



(GLDAS_NOAH025_M 2.1), taking monthly anomalies of SM up to a depth of 2 m, at 0.25° spatial resolution. The results of the correlations between piezometric data and TWS before and after subtraction of SM showed practically no significant difference. Moreover, no significant variation is observed graphically in the TWS curves before and after the subtraction of SM. These findings indicate that the contribution of SM to TWS is negligible. Figure 11 illustrates the correlation values obtained between TWS and piezometric data. According to the Pearson correlation indicator, the JPL dataset showed the best correlation with changes in groundwater levels.

Furthermore, the snow fraction does not exist in the study area, canopy values are negligible, and surface waters are mainly represented by anthropogenic hydraulic infrastructures, notably dams (Ouatiki et al., 2022). For the Sehouf aquifer, located near the SMBA dam, the median correlations vary from 0.58 for CSR, 0.71 for JPL, and 0.68 for TWS-Avr, which is considered high (Figure 11). Additionally, low biases (Shift between the piezometric curve and that of the CSR and JPL products) are observed for this aquifer (Figure 10A and Supplementary Figure S2). These results indicate that TWS is largely determined by the GWS in the study area, characterized as a semi-arid environment.

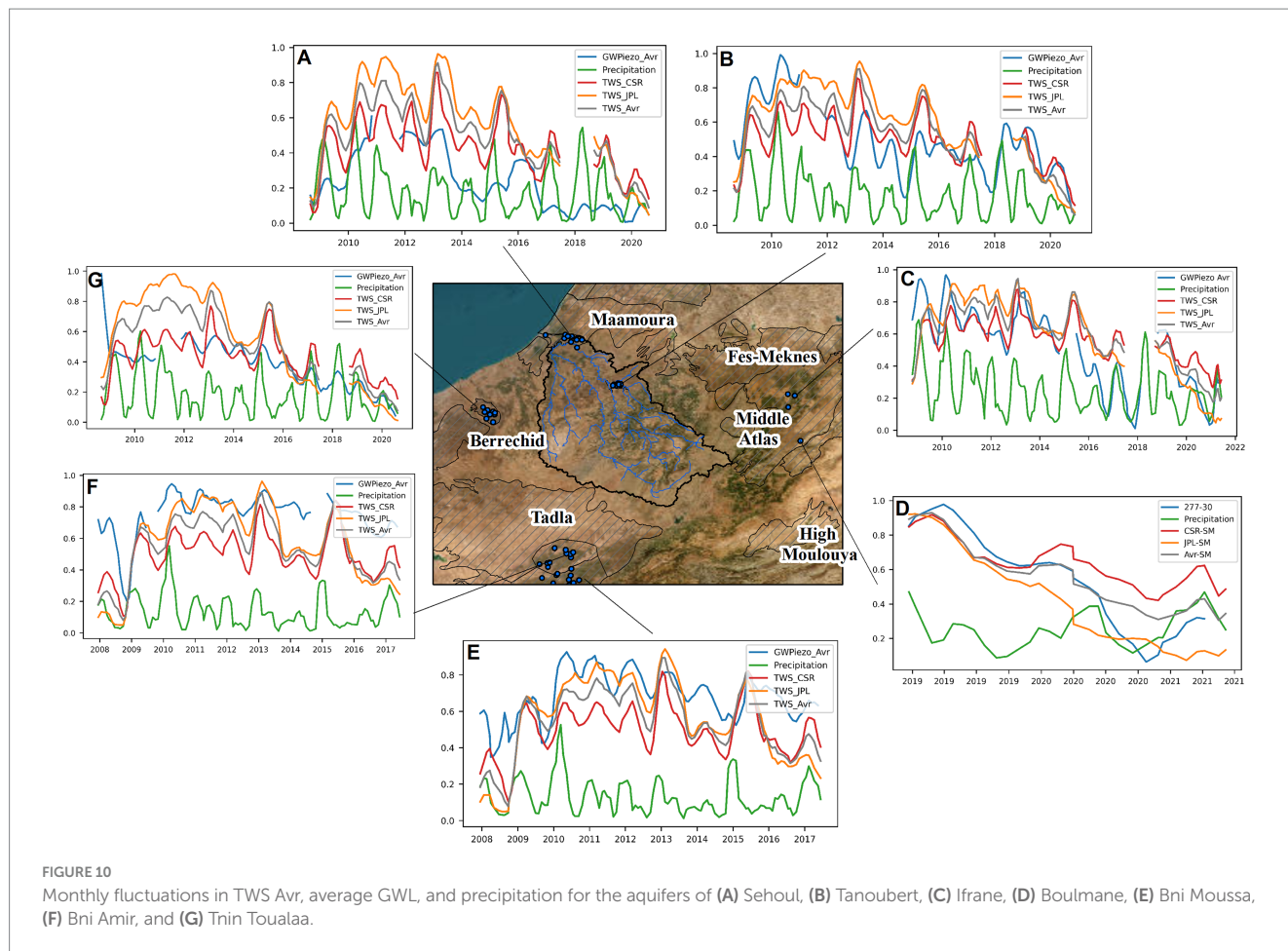
Finally, the results show that the maximum correlation between GWL and GRACE observations occurs with a one-month lag for the Tanoubert, Tnin Toualaa, Bni Moussa, and Ifrane-Boulmane aquifers, a two-month lag for the Sehouf aquifers, and a four-month lag for the Bni Amer aquifers. This time lag has been addressed in previous studies.

Pardo-Igúzquiza et al. (2023) explained the one-month lag by noting that variations in gravity are instant, whereas rainfall water takes about 1 month to travel through the vadose zone to reach the groundwater table. Neves et al. (2020) suggested that the 1- to 2-month delays in *in-situ* observations compared to satellite data are due to local hydrogeological properties and are not a uniform regional feature. According to Akhtar et al. (2022), the weak correlation between GRACE-derived groundwater storage anomalies (GWSA) and *in-situ* observations is attributed to a lag time of 3–4 months. Geomorphological complexity and landscape slope further exacerbate discrepancies. Moreover, applying spatially averaged GWSA on a monthly basis reduces the two datasets. Hence, caution is warranted when utilizing GRACE data in regions characterized by heterogeneous geomorphology.

3.4.2 Impact of drought on GWL

According to the results of the Mann-Kendall and Theil-Sen slope analyses, the three GRACE datasets examined (CSR, JPL, and Avr) exhibit similar behaviors in terms of the direction and magnitude of long-term trends. The findings show that downward trends (Sen's Slopes ≤ -0.007) in TWS are prevalent across the spatial domain, with high statistical significance (p -values $\leq 5.66E-06$, Significance threshold of 5%). In the subsequent analysis, the data used correspond to the average TWS estimates derived from the CSR and JPL GRACE mascon solutions. This choice is motivated by the fact that CSR data show the best consistency, while JPL data exhibit the best correlation.

Figure 12 illustrates the monthly variations in TWS estimates for each zone of interest. The areas exhibit similar TWS behavior, resulting

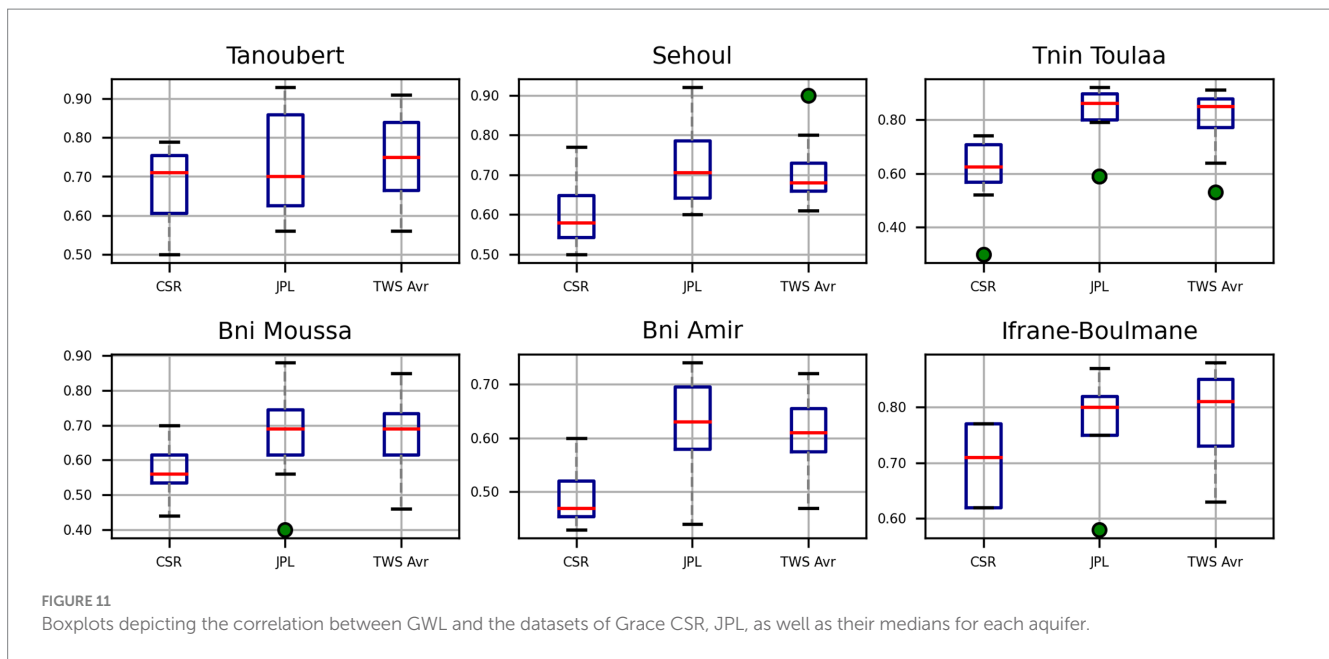


in comparable graphs and curves. This observed similarity can be attributed to several factors inherent to the GRACE data measurement and processing method: (a) Spatial resolution and smoothing effect: The GRACE-FO mascon data have a spatial resolution that, although improved compared to earlier versions, remains limited. GRACE-FO data, even at a resolution of $0.25 \times 0.25^\circ$, undergo spatial smoothing due to the mascon processing method. Hydrological signals are often smoothed to reduce the apparent variability on small spatial scales, which can lead to similarities and create homogeneity in TWS observations across nearby areas (Wiese et al., 2016; Tapley et al., 2019); (b) Data filtering and processing: GRACE-FO products involve the application of spatial and temporal filters to remove noise and systematic errors. The mascon method uses regularized solutions to improve the spatial resolution and accuracy of data. These filterings can contribute to high correlations between neighboring pixels (Save et al., 2016); (c) Consistent hydrological response: Regional hydrological variations may also show similar trends in geographically close areas due to common climatic and hydrological factors (Longuevergne et al., 2010; Rodell et al., 2018); (d) Watershed area: Our watershed of $9,642 \text{ km}^2$ is relatively homogeneous in size, allowing regional hydrological effects to be consistently visible across the studied areas. Additionally, this area is also subject to inherent limitations of the mascon method and the spatial resolution of the data; (e) Measurement error and uncertainty: GRACE-FO measurements involve uncertainties and measurement errors. Data processing techniques aim to minimize these errors, but

residual correlations remain, which can appear as similarities in the time series (Landerer and Cooley, 2021).

Furthermore, in terms of interpretation, it is important to note that while GRACE TWS provides valuable insights into regional water storage changes, analysis at a 0.25° resolution introduces an additional level of uncertainty. Such experimental sub-grid studies are useful for identifying and comparing initial trends, but they should not be regarded as highly localized hydrological assessments. This experimental approach highlights the need for caution, especially in complex and heterogeneous regions where spatial averaging may influence data interpretation.

The analysis of fluctuations in TWS estimates derived from GRACE Avr data over the period 2002–2023 highlights distinct phases across the entire study area. The first phase, from April 2002 to September 2008, is marked by a series of oscillations between periods of increase and decrease, but overall, a global decrease in TWS is observed (Figure 12). The second phase, from October 2008 to December 2012, shows an increase in TWS, notably significant in the northern part of the Bouregreg watershed, coinciding with a period of wet meteorological conditions. During this phase, water storage reaches high levels, with the peak recorded in December 2012. The third phase, spanning from January 2013 to January 2019, is characterized by a global decrease in TWS, surpassing the decline observed during the first phase. This third phase coincides with a notable increase in soil and air temperatures (Sections 3.1.3 and 3.2).



Finally, the last phase, from February 2019 to October 2023, is marked by a historical decrease in TWS, reaching unprecedented levels (Figure 12). The most affected zones are located in the southern part of the watershed, particularly around the Bni Moussa and Bni Amer aquifers, which experienced decreases of 0.198 cm/yr. and 0.183 cm/yr., respectively. Conversely, the Tnin-Toulaa aquifer was the least affected, with a decrease of 0.132 cm/yr. In between, the Tanoubert and Sehoul aquifers saw decreases of 0.182 cm/yr. and 0.179 cm/yr., respectively (Figure 13). In the Bouregreg watershed, the depletion in TWS can be estimated at 17.22 mm³/yr., with an average drop of 0.182 cm/yr. Overall, the negative trends of the Theil-Sen slope are statistically significant, with p -values $\leq 2.93E-01$.

These temperature increases lead to an increase in evapotranspiration in the study area, resulting in a water imbalance in the atmosphere and surface waters. This translates into a decrease in surface water availability, impacting recharge and groundwater. These conditions, combined with intensified groundwater overexploitation during drought periods, contribute to the accentuation of the observed decline in storage levels during the third and fourth phases (Figure 12).

Increases in temperatures lead to systematic changes in the balance between water and energy factors in terrestrial ecosystems (Siebert et al., 2015; Nilsson et al., 2005; Veldkamp et al., 2017). As temperatures rise, potential evapotranspiration (PET) also increases. With constant precipitation, these increases in PET directly result in increased aridity. The rise in PET exacerbates an already water-limited system by altering the balance between water supply and demand. This leads to transitions from moderately water- and energy-limited systems to strongly water-limited systems.

The surface and groundwater interactions fluxes are crucial for the dynamics of natural hydrological systems. With rising temperatures, an increase in evapotranspiration can divert a portion of the precipitation that would normally flow on the surface or infiltrate into the soil for recharge (Condon and Maxwell, 2019). This change in incoming flux can alter the long-term recharge patterns of hydrogeological systems. These modifications can influence groundwater levels and thus impact the groundwater and surface

water interactions, as well as soil moisture (Kustu et al., 2010; Yeh and Eltahir, 2005).

In the presence of a deep-water table, surface water typically replenishes the groundwater table; however, when groundwater is at a critical depth (<10 m), interactions between the water table and soil moisture can contribute to supporting evapotranspiration by capillarity (Kollet and Maxwell, 2008; Fan, 2015). An analysis of soil saturation at different depths, conducted by Yeh and Famiglietti (2009), confirms the predominance of groundwater evaporation in the water table during dry periods. Additionally, according to Condon and Maxwell (2019), in the wettest regions of the United States, the water table tends to be shallow and closely follows the topography, whereas in the drier western regions, groundwater is generally deeper. With increasing aridity due to climate change, groundwater depth is increasing throughout the region, indicating a systematic drying of the underground layers.

The GRACEDSI is defined as the normalized anomalies of TWS. It provides a perspective for comparing large-scale drought characteristics in space and time, without the limitations of more traditional monitoring methods. Figure 14 illustrates the spatiotemporal distribution of GRACEDSI in the region of interest. Overall, the results indicate a general downward trend, indicating increased drought, with high level of statistical significance (p value of 4.95E-10) (Figure 14).

3.4.3 Characterization of drought by GRACEDSI

The GRACEDSI data revealed that during the first phase, from April 2002 to September 2008, the study area experienced a succession of drought, humidity, and normal conditions. This period was characterized by a predominance of normal to dry conditions (GRACEDSI <0) across the area, particularly after 2005. Within this timeframe, 2004 was the wettest year (Figure 14).

Between October 2008 and January 2019, this period is globally humid, especially between October 2008 and December 2012, marked by abundant rainfall. This period is characterized by the predominance of normal and wet conditions. Spatially, there is an increase in

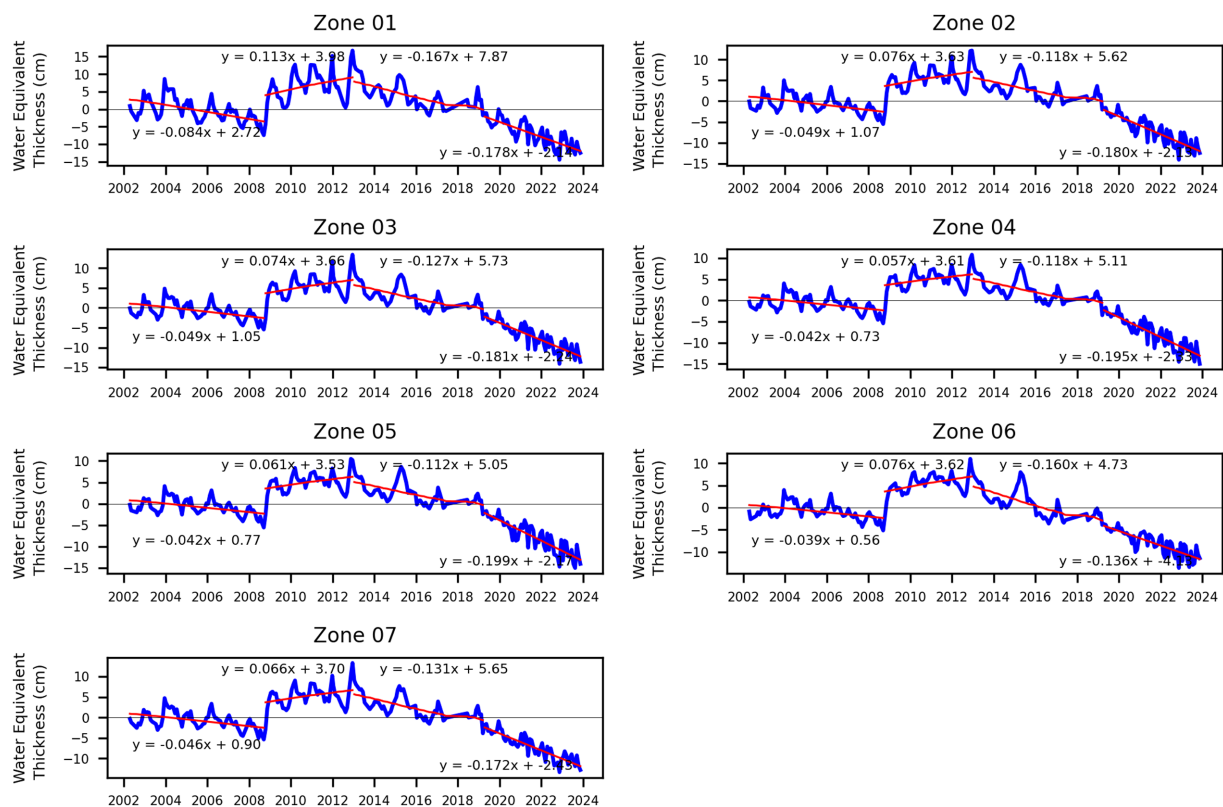


FIGURE 12
Monthly variations of TWS estimates in the region of interest.

humidity intensity moving from south to north of the area of interest and from west to east, with frequencies of “extremely wet” classes ($1.60 < \text{GRACEDSI} < 1.99$) and “exceptionally wet” ($\text{GRACEDSI} > 2$) ranging from 6.5% in the southwest to 17.4% in the northeast (Figures 5, 14).

Due to the cessation of the GRACE satellite mission in June 2017 and the launch of the GRACE Follow-On mission in May 2018, no data is available for the period from July 2017 to May 2018. Overall, the period between January 2013 and January 2019 was characterized by humidity where conditions from the previous period persisted. After 2013, conditions became increasingly less humid, and towards the end of the period, they became almost normal ($0 < \text{GRACEDSI} < 0.49$) (Figures 5, 14).

After January 2019, conditions evolved to become normal with a tendency towards drought. Over time, drought gradually intensified, signaling a shift towards extreme drought levels. No humid periods were recorded during this phase, resulting in a noticeable accumulation of drought (Figures 5, 14).

To analyze the relationship and evolution of GRACEDSI in relation to other indices, particularly SPEI and TCI, a spatiotemporal correlation analysis was conducted using Pearson correlation (Equation 10). This analysis aims to elucidate the connections between these different indicators and better understand the relationships between weather conditions and total water storage.

The results of this correlation show weak to moderate relationships between DRACEDSI and TCI, with values ranging from 0.15 to 0.50. This indicates that, although there are some common trends between

the two indices and a certain relationship exists, it is moderate and could be influenced by other factors not captured in this analysis, particularly anthropogenic effects. Weak correlations were found between GRACEDSI and SPEI, with values varying from 0.05 to 0.21. These low correlation values suggest that GRACEDSI and SPEI are weakly associated and not directly linked. Moreover, moderate to strong correlations were observed between SPEI and TCI, with values ranging from 0.37 to 0.62 (Section 3.3), indicating a more significant association compared to the other pairs of indices.

In conclusion, this combination of results suggests an increased risk of drought, attributable to higher temperatures that promote evapotranspiration, leading to a water imbalance affecting surface and groundwater resources. This situation is exacerbated by the growing demand for water due to population growth, improved living standards, and increasing industrialization (Figures 5, 14).

3.5 Environmental protection and climate change

The sustainability of the natural environment depends on the provision of ecosystem goods and services, which are influenced by both natural and anthropogenic factors (European Commission, 2009; Millennium Ecosystem Assessment, 2005). Climate change, particularly drought, has a significant impact on the ecosystems of arid and semi-arid regions (Keshavarz and Karami, 2016). Morocco's economic and social development heavily relies on water resource exploitation, with irrigated agriculture consuming an average of 85%

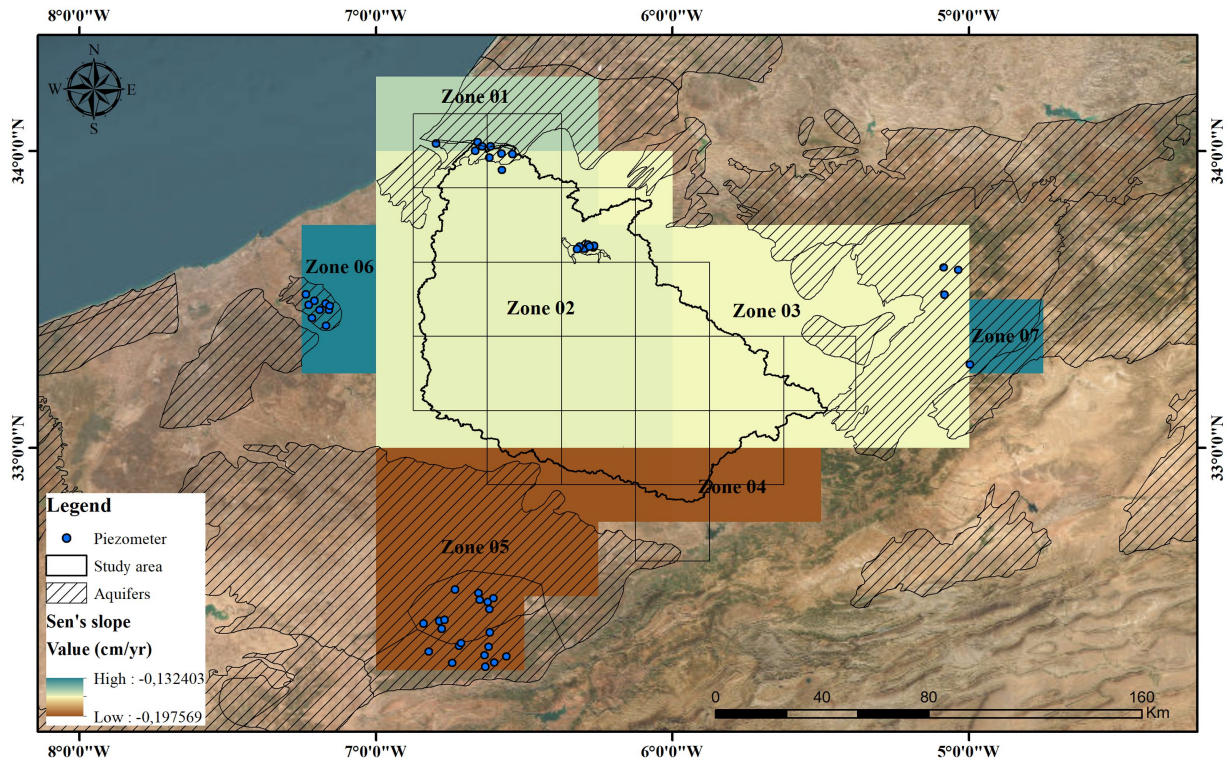


FIGURE 13 Trends estimated using the Theil-Sen slope estimator for the period from 2019 to October 2023.

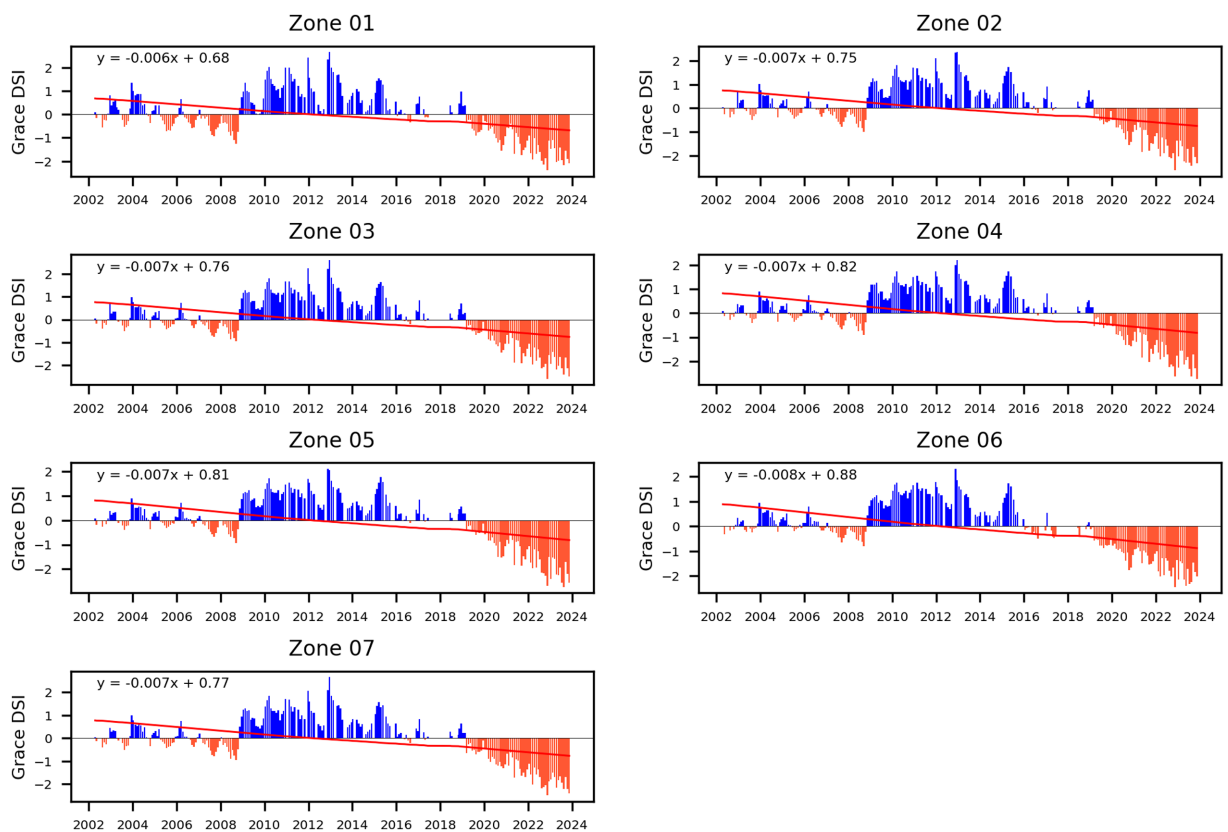


FIGURE 14 Drought's spatiotemporal evolution using the GRACEDSI monthly in the region of interest, as well as the regions encompassing the piezometers used in this study.

of available water resources, while public water supply and industry use 12 and 3%, respectively (Ouassou et al., 2005; MEE, 2015). This study highlights the importance of addressing the multifaceted impacts of drought on natural ecosystems and human systems, emphasizing the effects on agriculture, soils, vegetation, and water resource management.

In the study area, drought has become structural, placing pressure on water resources by increasing the demand related to evapotranspiration, which affects water reserves, recharge, and soil moisture, thereby exacerbating water scarcity issues and threatening food security (Belcaid and El Ghini, 2020; Meliho et al., 2020; El Khatri and El Hairech, 2014). Water scarcity leads to a reduction in irrigated areas (Melihio et al., 2020; Guemouria et al., 2023), a decrease in cereal production (wheat and barley), forage stocks, and degradation of pasture biomass (Lebdi and Maki, 2023; Berkat and Tazi, 2006; Verner et al., 2018). The variation in major cereal production is closely related to SPEI and TCI indices (Gumus et al., 2024; Hakam et al., 2023). Additionally, the relationship between the Standardized Precipitation Evapotranspiration Index (SPEI) and the Temperature Condition Index (TCI) with soil health and degradation has been explored in various studies (Sun et al., 2020; Lee, 2021; Jung et al., 2023).

High temperatures and increased evapotranspiration significantly impact natural ecosystems, particularly forests and wetlands. More intense evapotranspiration reduces soil and vegetation water availability, stressing forest ecosystems and affecting tree growth and health (Zhu et al., 2024; Liu et al., 2022; Brockerhoff et al., 2017; Xu et al., 2014). In wetlands, these conditions can lower water levels, disrupting the hydrological balance and potentially degrading these ecosystems (Yang et al., 2015; Zhou et al., 2020).

The implications of this study in terms of climate change primarily include hydrological imbalance, increased aridity, and heightened risk of drought. Water is the main vector through which climate change affects the ecosystem and the inhabitants of the Earth (UNWWAP, 2009). Long-term changes in evaporation and potential evapotranspiration can have profound repercussions on hydrological processes and the agricultural system. The meteorological parameters responsible for these changes are well identified (Sarker, 2022; Gurara et al., 2021; Helfer et al., 2012). Such changes can have significant consequences for economic and environmental well-being, especially if the increase in evaporation is not compensated by an adequate increase in precipitation (Chattopadhyay and Hulme, 1997). Furthermore, the divergence between changes in atmospheric and ecohydrological aridity can be primarily attributed to moisture limitations from dry soils and the physiological regulations of plant evapotranspiration under climate warming (Lian et al., 2021; Sarker, 2022).

Groundwater plays a crucial role in maintaining ecosystems and human adaptation to environmental changes, while surface water systems are becoming increasingly unsustainable in the face of climate change (Liesch and Wunsch, 2019; Rafik et al., 2023a,b). In the study area, the decline in groundwater levels and the decrease in aquifers highlight the vulnerability of water resources to climate change, both in terms of quantity and quality. Effective water management strategies are essential to address these challenges and ensure a sustainable water supply.

This study emphasizes the importance of integrated water resources management (IWRM) to ensure food, water, and energy

security. The chapter addresses the efficient use of water, policies to combat climate change and drought, the exploitation of unconventional water resources, and stakeholder participation (Le Page et al., 2020; Ben-Daoud et al., 2021, 2023; Banouar and Bouslihim, 2024; Benchbani et al., 2022; Rbaibi and SahibEddine, 2024; Lenton, 2011; Giordano and Shah, 2014).

4 Conclusions and perspectives

The Bouregreg watershed represents a typical example of a region characterized by arid and semi-arid conditions, exposed to climate change due to its position in the Mediterranean zone. Drought has a significant impact on the development of this area. This article aims to characterize drought in terms of spatial and temporal configuration, using different drought indices.

The main conclusion of this study reveals an alternation between periods of drought and humidity, with a significant overall trend towards decrease, indicating that the entire study area is prone to drought ranging from moderate to extreme. These findings also demonstrate that the observed decrease is linked to an increase in evapotranspiration (SPEI), particularly after 2010, in response to rising temperatures (STI and TCI). However, SPI has shown relative stability, suggesting little notable changes in precipitation. This underscores the importance of employing multiple indices simultaneously to comprehensively assess drought conditions in a given region.

Moreover, DSI results, based on Total Water Storage (TWS) GRACE data, highlight a significant storage loss attributed to changes in the hydrological system, exchanges between surface and groundwater and other anthropogenic factors in recent years. While the experimental approach using GRACE TWS data at a 0.25-degree resolution can provide valuable insights, it requires further validation before being considered conclusive. The implications of these results should be discussed with an awareness of the provisional nature of the data.

Furthermore, correlation analyses have revealed relatively strong positive relationships between SPEI and SPI, between TCI and STI as well as between SPEI and TCI. These results underscore a robust association between evapotranspiration fluctuations and temperature variations. Additionally, weak to moderate correlations were observed between GRACEDSI and TCI, suggesting that there are some common trends between the two indices and a moderate relationship influenced by other factors not included in the analysis.

In summary, the results underscore that the entire studied area is exposed to drought risks, attributed to increasing evapotranspiration rates. This rise leads to a decrease in surface water availability, thereby impacting recharge and groundwater reserves. However, while evapotranspiration exerts a significant influence on surface and groundwater reserves, human impact remains significant. The human impact on hydrological systems is evident through an increasing demand for water due to the expansion of irrigated agriculture, changes in river flow regimes, and hydrological disconnection caused by the construction of dams that hinder groundwater recharge. This situation leads to a cascade of water shortages due to human activities. Therefore, it is essential to assess this aspect to obtain a more comprehensive and robust understanding of the climatic and environmental conditions in the study area.

Data availability statement

The datasets presented in this study can be found in online repositories. The names of the repository/repositories and accession number(s) can be found in the article/[Supplementary material](#).

Author contributions

LAD: Conceptualization, Data curation, Formal analysis, Investigation, Methodology, Project administration, Resources, Software, Supervision, Validation, Visualization, Writing – original draft, Writing – review & editing. MES: Conceptualization, Formal analysis, Methodology, Supervision, Validation, Visualization, Writing – original draft, Writing – review & editing. JM: Conceptualization, Formal analysis, Methodology, Resources, Supervision, Validation, Visualization, Writing – original draft, Writing – review & editing. AR: Data curation, Methodology, Writing – original draft, Writing – review & editing. AH: Conceptualization, Formal analysis, Funding acquisition, Investigation, Methodology, Resources, Supervision, Validation, Visualization, Writing – original draft, Writing – review & editing.

Funding

The author(s) declare that financial support was received for the research, authorship, and/or publication of this article. This research was funded by the UM6P (Mohammed VI Polytechnic University) through the starting grant of Abdessamad Hadri.

References

- Abdi-Dehkordi, M., Bozorg-Haddad, O., Salavitarab, A., Mohammad-Azari, S., and Goharian, E. (2021). Development of flood mitigation strategies toward sustainable development. *Nat. Hazards* 108, 2543–2567. doi: 10.1007/s11069-021-04788-5
- Agha-Kouchak, A., Farahmand, A., Melton, F. S., Teixeira, J., Anderson, M. C., Wardlaw, B. D., et al. (2015). Remote sensing of drought: Progress, challenges and opportunities. *Rev. Geophys.* 53, 452–480. doi: 10.1002/2014RG000456
- Aires, F., Prigent, C., Rossow, W. B., and Rothstein, M. (2001). A new neural network approach including first-guess for retrieval of atmospheric water vapor, cloud liquid water path, surface temperature and emissivities over land from satellite microwave observations. *J. Geophys. Res.* 106, 14887–14907. doi: 10.1029/2001JD900085
- Ait Dhmane, L., Moustadraf, J., Rachdane, M., Saidi, M. E., Benjmel, K., Amraoui, F., et al. (2023). Spatiotemporal assessment and correction of gridded precipitation products in North Western Morocco. *Atmosphere* 14:1239. doi: 10.3390/atmos14081239
- Akhtar, F., Nawaz, R. A., Hafeez, M., Awan, U. K., Borgemeister, C., and Tischbein, B. (2022). Evaluation of GRACE derived groundwater storage changes in different agro-ecological zones of the Indus Basin. *J. Hydrol.* 605:127369. doi: 10.1016/j.jhydrol.2021.127369
- Allen, P. M., Harmel, R. D., Dunbar, J. A., and Arnold, J. G. (2011). Upland contribution of sediment and runoff during extreme drought: A study of the 1947–1956 drought in the Blackland prairie, Texas. *J. Hydrol.* 407, 1–11. doi: 10.1016/j.jhydrol.2011.04.039
- Allen, R. G., Pereira, L. S., Raes, D., and Smith, M. (1998). Crop evapotranspiration – guidelines for computing crop water requirements. In: *Irrigation and drain*, paper no. 56. FAO, Rome, Italy, 300 pp.
- Amjath-Babu, T. S., Sharma, B., Brouwer, R., Rasul, G., Wahid, S. M., Neupane, N., et al. (2019). Integrated modelling of the impacts of hydropower projects on the water-food-energy nexus in a transboundary Himalayan river basin. *Appl. Energy* 239, 494–503. doi: 10.1016/j.apenergy.2019.01.147
- Banerjee, C., and Kumar, D. N. (2018). Analyzing large-scale hydrologic processes using GRACE and hydrometeorological datasets. *Water Resour. Manag.* 32, 4409–4423. doi: 10.1007/s11269-018-2070-x
- Banouar, A., and Bouslih, A. (2024). Integrated water resource management in the decision-making of large firms in Morocco: case of Managem group (hydraulic basin of Tensift AL Haouz). *E3S Web Conf.* 489:05001. doi: 10.1051/e3sconf/202448905001
- Barrett, E., Beaumont, M., and Herschy, R. (1990). Satellite remote sensing for operational hydrology: present needs and future opportunities. *Remote Sens. Rev.* 4, 451–466. doi: 10.1080/02757259009532113
- Beguieria, S., and Vicente-Serrano, S. (2009). DIGITAL.CSIC. Récupéré sur SPEI Calculator.
- Belcaid, K., and El Ghini, A. (2020). “Measuring the weather variability effects on the agricultural sector in Morocco” in Proceedings of the Thirteenth International Conference on Management Science and Engineering Management. ICMSEM 2019. Advances in Intelligent Systems and Computing, vol. 1001. eds. J. Xu, S. Ahmed, F. Cooke and G. Duca (Springer, Cham).
- Benchbani, I., Sebari, K., and Zemzami, M. (2022). Integrated water resources management in the Loukkos basin (Morocco): an approach to improve resilience under climate change impact. *E3S Web of Conferences* 346:03024. doi: 10.1051/e3sconf/202234603024
- Ben-Daoud, M., El Mahrad, B., Elhassnaoui, I., Moumen, A., Sayad, A., Elboughadioui, M., et al. (2021). Integrated water resources management: an indicator framework for water management system assessment in the R'Dom sub-basin, Morocco. *Environ. Chall.* 3:100062. doi: 10.1016/j.envc.2021.100062
- Ben-Daoud, M., El Mahrad, B., Moroşanu, G. A., Ben-Daoud, A., Mon, S. W., Elhassnaoui, I., et al. (2023). Water resources planning and management: from stakeholders' local actions to the global perspective. *Sustain. Water Resour. Manage.* 9:132. doi: 10.1007/s40899-023-00919-x
- Bento, V., Trigo, I., Gouveia, C., and DaCamara, C. (2018). Contribution of land surface temperature (T_{CI}) to vegetation health index: A comparative study using clear sky and all-weather climate data records. *Remote Sens.* 10:1324. doi: 10.3390/rs10091324
- Berkat, O., and Tazi, M. (2006). Country pasture/forage resource profiles: Morocco. FAO, Rome. Available at: http://www.fao.org/ag/agp/agpc/doc/counprof/PDF%2520files/SouthAfrica_English.pdf.

Acknowledgments

The authors would like to express their gratitude to the Bouregreg and Chaouia Hydraulic, Sebou and Oum Er-Rabia Basin Agencies for providing the ground data required for this study and to UM6P (Mohammed VI Polytechnic University) for the financial support. We also thank the editor and reviewers for their time.

Conflict of interest

The authors declare that the research was conducted in the absence of any commercial or financial relationships that could be construed as a potential conflict of interest.

Publisher's note

All claims expressed in this article are solely those of the authors and do not necessarily represent those of their affiliated organizations, or those of the publisher, the editors and the reviewers. Any product that may be evaluated in this article, or claim that may be made by its manufacturer, is not guaranteed or endorsed by the publisher.

Supplementary material

The Supplementary material for this article can be found online at: <https://www.frontiersin.org/articles/10.3389/frwa.2024.1463748/full#supplementary-material>

- Boughdadi, S., Ait Brahim, Y., El Alaoui El Fels, A., and Saidi, M. E. (2023). Rainfall variability and teleconnections with large-scale atmospheric circulation patterns in west-Central Morocco. *Atmos.* 14:1293. doi: 10.3390/atmos14081293
- Brockerhoff, E. G., Barbaro, L., Castagneyrol, B., Forrester, D. I., Gardiner, B., González-Olabarria, J. R., et al. (2017). Forest biodiversity, ecosystem functioning and the provision of ecosystem services. *Biodivers. Conserv.* 26, 3005–3035. doi: 10.1007/s10531-017-1453-2
- Brouziyne, Y., Abouabdillah, A., Chehbouni, A., Hanich, L., Bergaoui, K., McDonnell, R., et al. (2020). Assessing hydrological vulnerability to future droughts in a Mediterranean watershed: combined indices-based and distributed modeling approaches. *Water* 12:2333. doi: 10.3390/w12092333
- Chattopadhyay, N., and Hulme, M. (1997). Evaporation and potential evapotranspiration in India under conditions of recent and future climate change. *Agric. For. Meteorol.* 87, 55–73. doi: 10.1016/S0168-1923(97)00066-3
- Chen, J. L., Wilson, C. R., Tapley, B. D., Yang, Z. L., and Niu, G. Y. (2009). 2005 drought event in the Amazon River basin as measured by GRACE and estimated by climate models. *J. Geophys. Res.* 114:B05404. doi: 10.1029/2008JB006056
- Chiaravalloti, F., Brocca, L., Procopio, A., Massari, C., and Gabriele, S. (2018). Assessment of GPM and SM2RAIN-ASCAT rainfall products over complex terrain in southern Italy. *Atmos. Res.* 206, 64–74. doi: 10.1016/j.atmosres.2018.02.019
- Condon, L. E., and Maxwell, R. M. (2019). Simulating the sensitivity of evapotranspiration and streamflow to large-scale groundwater depletion. *Sci. Adv.* 5:eav4574. doi: 10.1126/sciadv.aav4574
- Cos, J., Doblas-Reyes, F., Jury, M., Marcos, R., Bretonnière, P. A., and Samsó, M. (2022). The Mediterranean climate change hotspot in the CMIP5 and CMIP6 projections. *Earth Syst. Dynam.* 13, 321–340. doi: 10.5194/esd-13-321-2022
- Dai, A. (2010). Drought under global warming: A review. *Wiley Interdiscip. Rev. Clim. Chang.* 2, 45–65. doi: 10.1002/wcc.81
- Darabi, H., Danandeh Mehr, A., Kum, G., Sönmez, M. E., Dumitrache, C. A., Diani, K., et al. (2023). Hydroclimatic trends and drought risk assessment in the Ceyhan River basin: insights from SPI and STI indices. *Hydrology* 10:157. doi: 10.3390/hydrology10080157
- Doorenbos, J., and Pruitt, W. O. (1977). Crop water requirements. In: FAO irrigation and drainage paper no. 24. Food and agriculture Organization of the United Nations, Rome, 144 pp.
- el Alaoui el Fels, A., Saidi, M. E., and Alam, M. J. B. (2022). Rainfall frequency analysis using assessed and corrected satellite precipitation products in Moroccan arid areas. The case of Tensift watershed. *Earth Syst. Environ.* 6, 391–404. doi: 10.1007/s41748-021-00290-x
- El Aoula, R., Mahé, G., Mhammdi, N., Ezzahouani, A., Kacimi, I., and Khomsi, K. (2021). Evolution of the hydrological regime in the Bouregreg watershed, Morocco. *Proc. IAHS* 384, 163–168. doi: 10.5194/piahs-384-163-2021
- El Khatri, S., and El Hairech, T. (2014). Drought conditions and management strategies in Morocco. Casablanca: Direction de la Météorologie Nationale.
- el Mezouary, L., Hadri, A., Kharrou, M. H., Fakir, Y., Elfarchouni, A., Bouchaou, L., et al. (2024). Contribution to advancing aquifer geometric mapping using machine learning and deep learning techniques: a case study of the AL Haouz-Mejjate aquifer, Marrakech, Morocco. *Appl. Water Sci.* 14:102. doi: 10.1007/s13201-024-02162-x
- Elair, C., Rkha, C. K., and Hadri, A. (2023). Assessment of drought variability in the Marrakech-Safi region (Morocco) at different time scales using GIS and remote sensing. *Water Supply* 23, 4592–4624. doi: 10.2166/ws.2023.283
- Elkharrim, M., and Bahi, L. (2014). Using statistical downscaling of GCM simulations to assess climate change impacts on drought conditions in the northwest of Morocco. *Mod. Appl. Sci.* 9, 1–11. doi: 10.5539/mas.v9n2p1
- Er-Raki, S., Chehbouni, A., Khabba, S., Simonneaux, V., Jarlan, L., Ouldabba, A., et al. (2010). Assessment of reference evapotranspiration methods in semi-arid regions: can weather forecast data be used as alternate of ground meteorological parameters? *J. Arid Environ.* 74, 1587–1596. doi: 10.1016/j.jaridenv.2010.07.002
- European Commission (2009). Ecosystem goods and services. Available at: <http://ec.europa.eu/environment/nature/info/pubs/docs/ecosystem.Pdf>
- Fan, Y. (2015). Groundwater in the Earth's critical zone: relevance to large-scale patterns and processes. *Water Resour. Res.* 51, 3052–3069. doi: 10.1002/2015WR017037
- Feng, S., Hao, Z., Wu, X., Zhang, X., and Hao, F. (2021). A multi-index evaluation of changes in compound dry and hot events of global maize areas. *J. Hydrol.* 602:126728. doi: 10.1016/j.jhydrol.2021.126728
- Fniguire, F., Laftouhi, N. E., Saidi, M. E., Zamrane, Z., El Himer, H., and Khalil, N. (2017). Spatial and temporal analysis of the drought vulnerability and risks over eight decades in a semi-arid region (Tensift basin: Morocco). *Theor. Appl. Climatol.* 130, 321–330. doi: 10.1007/s00704-016-1873-z
- Gao, Y., Sarker, S., Sarker, T., and Leta, O. T. (2022). Analyzing the critical locations in response of constructed and planned dams on the Mekong River basin for environmental integrity. *Environ. Res. Commun.* 4:101001. doi: 10.1088/2515-7620/ac9459
- GeoAtlas, (2009). Geophysical study of the Thine Toualaa aquifer Ben Slimane province. Study Report; Hydraulic Basin Agency of Bouregreg and Chaouia: Benslimane, Morocco; 13 pp.
- Ghaleb, F., Mario, M., and Sandra, A. (2015). Regional landsat-based drought monitoring from 1982 to 2014. *Climate* 3, 563–577. doi: 10.3390/cli3030563
- Giordano, M., and Shah, T. (2014). From IWRM back to integrated water resources management. *Int. J. Water Resour. Dev.* 30, 364–376. doi: 10.1080/07900627.2013.851521
- Gold, L. W. (1967). Influence of surface conditions on ground temperatures. *Can. J. Earth Sci.* 4, 199–208. doi: 10.1139/e67-010
- Guemouria, A., El Harraki, W., Elhassnaoui, I., Hadri, A., Chehbouni, A., Dhiba, D., et al. (2023). Opportunities and challenges of irrigation in Morocco, Spain, and India: A critical analysis. *World Water Policy* 9, 682–701. doi: 10.1002/wwp2.12148
- Gumus, V., El Moçayd, N., Seker, M., and Seaid, M. (2024). Future projection of droughts in Morocco and potential impact on agriculture. *J. Environ. Manag.* 367:122019. doi: 10.1016/j.jenvman.2024.122019
- Gurara, M. A., Jilo, N. B., and Tolche, A. D. (2021). Impact of climate change on potential evapotranspiration and crop water requirement in upper Wabe bridge watershed, Wabe Shebele River basin, Ethiopia. *J. Afr. Earth Sci.* 180:104223. doi: 10.1016/j.jafrearsci.2021.104223
- Hadri, A., Saidi, M. E. M., and Boudhar, A. (2021a). Multiscale drought monitoring and comparison using remote sensing in a Mediterranean arid region: A case study from west-Central Morocco. *Arab. J. Geosci.* 14:118. doi: 10.1007/s12517-021-06493-w
- Hadri, A., Saidi, M. E. M., El Khalki, E. M., Aachrine, B., Saouabe, T., and Elmaki, A. A. (2022). Integrated water management under climate change through the application of the WEAP model in a Mediterranean arid region. *J. Water Clim. Change* 13, 2414–2442. doi: 10.2166/wcc.2022.039
- Hadri, A., Saidi, M. E. M., Saouabe, T., and El Alaoui El Fels, A. (2021b). Temporal trends in extreme temperature and precipitation events in an arid area: case of Chichaoua Mejjate region (Morocco). *J. Water Clim. Change* 12, 895–915. doi: 10.2166/wcc.2020.234
- Hadria, R., Boudhar, A., Ouati, H., Lebrini, Y., Elmansouri, L., Gadouali, F., et al. (2019). Combining use of TRMM and ground observations of annual precipitations for meteorological drought trends monitoring in Morocco. *Am. J. Remote Sensing* 7:25. doi: 10.11648/j.ajrs.20190702.11
- Hakam, O., Baali, A., Azenoud, K., Lyazidi, A., and Bourchachen, M. (2023). Assessments of drought effects on plant production using satellite remote sensing technology, GIS and observed climate data in Northwest Morocco, case of the lower Sebou Basin. *Int. J. Plant Prod.* 17, 267–282. doi: 10.1007/s42106-023-00236-5
- Hanadé Houmma, I., El Mansouri, L., Gadal, S., Mamane Barkawi, M. B., and Hadria, R. (2022). Prospective analysis of spatial heterogeneity influence on the concordance of remote sensing drought indices: A case of semi-arid agrosystems in Morocco (Moulouya and Tensift watersheds). *Geocarto Int.* 37, 14899–14924. doi: 10.1080/10106049.2022.2092219
- Hansen, J., Sato, M., and Ruedy, R. (2012). Perception of climate change. *Proc. Natl. Acad. Sci. USA* 109, E2415–E2423. doi: 10.1073/pnas.1205276109
- Hao, C., Zhang, J., and Yao, F. (2015). Combinaison de données de télédétection multi-capteurs pour la surveillance de la sécheresse dans le sud-ouest de la Chine. *Int. J. Appl. Earth Obs. Geoinf.* 35, 270–283. doi: 10.1016/j.jag.2014.09.011
- Hargreaves, G. H., and Samani, Z. A. (1985). Reference crop evapotranspiration from temperature. *Appl. Eng. Agric.* 1, 96–99. doi: 10.13031/2013.26773
- Hayes, M. J., Alvord, C., and Lowrey, J. (2006). Indices de sécheresse. *Intermountain West Clim. Resume* 3, 2–6.
- Hayes, M., Svoboda, M., Wall, N., and Widhalm, M. (2011). The Lincoln declaration on drought indices: universal meteorological drought index recommended. *Bull. Am. Meteorol. Soc.* 92, 485–488. doi: 10.1175/2010BAMS3103.1
- HBABC (2019). Updating study of the master plan for the integrated development of water resources in the Bouregreg and Chaouia Hydraulic Basin. Mission 1: inventory, quantitative and qualitative assessment of water resources and state of the use of water resources. Sub-Mission 1.2: Quantitative assessment of water resources—Surface water resources component—Study report; Hydraulic Basin Agency of Bouregreg and Chaouia: Benslimane, Morocco; 155p.
- HBAOER (2007). Modeling study of the deep water tables of the Tadla, Mission I: Hydrogeological synthesis and updating of data relating to the deep water tables of the TADLA, Hydraulic basin Agency of Oum Er Rbia, Morocco.
- Helfer, F., Lemckert, C., and Zhang, H. (2012). Impacts of climate change on temperature and evaporation from a large reservoir in Australia. *J. Hydrol.* 475, 365–378. doi: 10.1016/j.jhydrol.2012.10.008
- Hersbach, H., Bell, B., Berrisford, P., Hirahara, S., Horányi, A., Muñoz-Sabater, J., et al. (2020). The ERA5 global reanalysis. *QJR Meteorol. Soc.* 146, 1999–2049. doi: 10.1002/qj.3803
- Heumann, B. W. (2011). Satellite remote sensing of mangrove forests: recent advances and future opportunities. *Prog. Phys. Geogr.* 35, 87–108. doi: 10.1177/0309133310385371
- Holzman, M. E., Rivas, R. E., and Bayala, M. I. (2021). Relationship between TIR and NIR-SWIR as Indicator of vegetation water availability. *Remote Sens.* 13:3371. doi: 10.3390/rs13173371
- IPCC. (2021) The physical science basis, climate change 2021. Contribution of working group I to the sixth assessment report of the intergovernmental panel on climate change.

- Jackson, R. D., Idso, S. B., Reginato, R. J., and Pinter, P. J. (1981). Canopy temperature as a crop water stress Indicator. *Water Resour. Res.* 17, 1133–1138. doi: 10.1029/WR017i004p01133
- Jamro, S., Channa, F. N., Dars, G. H., Ansari, K., and Krakauer, N. Y. (2020). Exploring the evolution of drought characteristics in Balochistan, Pakistan. *Appl. Sci.* 10:913. doi: 10.3390/app10030913
- Jiang, J., and Zhou, T. (2021). Human-induced rainfall reduction in drought-prone northern Central Asia. *Geophys. Res. Lett.* 48:e2020GL092156. doi: 10.1029/2020GL092156
- Jung, H., Won, J., Kang, S., and Kim, S. (2023). Spatiotemporal variability of vegetation response to meteorological drought on the Korean peninsula. *Hydrol. Res.* 54, 1625–1640. doi: 10.2166/nh.2023.237
- Kendall, M. (1975). Rank correlation measures. London: Charles Griffin, 15.
- Keshavarz, M., and Karami, E. (2016). Farmers' pro-environmental behaviour under drought: application of protection motivation theory. *J. Arid Environ.* 127, 128–136. doi: 10.1016/j.jaridenv.2015.11.010
- Khattabi, A., and Samira, B. (2006). Usages et activités humaines du bassin versant Bouregreg. 14th International Soil Conservation Organization Conference. Water Management and Soil Conservation in Semi-Arid Environments, Marrakech, Morocco, May 14–19, 2006 (ISCO 2006).
- Khomsi, K., Mahe, G., Sinan, M., and Snoussi, M. (2013). Evolution des Evenements Chauds Rares dans les Bassins Versants de Tensift et Bouregreg (Maroc) et Identification des Types de Temps Synoptiques Associés. In Reunion Multi-Acteurs, Sur le Bassin du Bouregreg; CERGeo: Rabat, Morocco.
- Knouz, N., Boudhar, A., Bachaoui, E. M., and Aghzaf, B. (2016). Study of the vulnerability of groundwater to pollution in semi-arid zones: case of the Béni Amir water table in Morocco. *Mediterranean. doi:* 10.4000/mediterranean.7853
- Kogan, F. N. (1995). Application of vegetation index and brightness temperature for drought detection. *Adv. Space Res.* 15, 91–100. doi: 10.1016/0273-1177(95)00079-T
- Kogan, F. N. (2000). Contribution of remote sensing to drought early warning. In: Early warning Systems for Drought Preparedness and Drought Management. Proceedings of an expert group meeting held, Lisbon, Portugal.
- Kollet, S. J., and Maxwell, R. M. (2008). Capturing the influence of groundwater dynamics on land surface processes using an integrated, distributed watershed model. *Water Resour. Res.* 44:W02402. doi: 10.1029/2007WR006004
- Krajewski, W. F., Anderson, M. C., Eichinger, W. E., Entekhabi, D., Hornbuckle, B. K., Houser, P. R., et al. (2006). A remote sensing observatory for hydrologic sciences: A genesis for scaling to continental hydrology. *Water Resour. Res.* 42:W07301. doi: 10.1029/2005WR004435
- Kramer, P. J. (1980). "Drought, stress, and the origin of adaptations" in Adaptations of plants to water and high temperature stress. eds. N. C. Turner and P. J. Kramer (New York: John-Wiley & Sons), 7–20.
- Kustu, M. D., Fan, Y., and Robock, A. (2010). Large-scale water cycle perturbation due to irrigation pumping in the US high plains: A synthesis of observed streamflow changes. *J. Hydrol.* 390, 222–244. doi: 10.1016/j.jhydrol.2010.06.045
- Landerer, F. W., and Cooley, S. S. (2021). GRACE-FO Level-3 data product user handbook, California.
- Landerer, F. W., and Swenson, S. C. (2012). Accuracy of scaled GRACE terrestrial water storage estimates. *Water Resour. Res.* 48. doi: 10.1029/2011WR011453
- Le Page, M., Fakir, Y., and Aouissi, J. (2020). "Chapter 7—Modeling for integrated water resources management in the Mediterranean region" in Water resources in the Mediterranean region. eds. M. Zribi, L. Brocca, Y. Trambay and F. Mollé (Amsterdam, The Netherlands: Elsevier), 157–190.
- Lebdi, F., and Maki, A. (2023). MOROCCO: FAO – La sécheresse au Maghreb: diagnostic, impacts et perspectives pour le renforcement de la résilience du secteur agricole. Available at: <https://openknowledge.fao.org/handle/20.500.14283/CC7126FR>
- Lee, Y. (2021). Development of integrated crop drought index by combining rainfall, land surface temperature, evapotranspiration, soil moisture, and vegetation index for agricultural drought monitoring. *Remote Sens.* 13:1778. doi: 10.3390/rs13091778
- Lee, S. H., Yoo, S. H., Choi, J. Y., and Bae, S. (2017). Assessment of the impact of climate change on drought characteristics in the Hwanghae plain, North Korea using time series SPI and SPEI: 1981–2100. *Water* 9:579. doi: 10.3390/w9080579
- Lenton, R. (2011). Integrated water resources management. Treatise on water science. Amsterdam: Elsevier, 9–21.
- Li, X., Chen, Y., Wang, H., and Zhang, Y. (2020). Assessment of GPM IMERG and radar quantitative precipitation estimation (QPE) products using dense rain gauge observations in the Guangdong-Hong Kong-Macao Greater Bay Area, China. *Atmos. Res.* 236:104834. doi: 10.1016/j.atmosres.2019.104834
- Li, J., Wang, Z., Wu, X., Zscheischler, J., Guo, S., and Chen, X. (2021). A standardized index for assessing sub-monthly compound dry and hot conditions. *Hydrol. Earth Syst. Sci.* 25, 1587–1601. doi: 10.5194/hess-25-1587-2021
- Lian, X., Piao, S., Chen, A., Huntingford, C., Fu, B., Li, L. Z. X., et al. (2021). Multifaceted characteristics of dryland aridity changes in a warming world. *Nat. Rev. Earth Environ.* 2, 232–250. doi: 10.1038/s43017-021-00144-0
- Liesch, T., and Wunsch, A. (2019). Aquifer responses to long-term climatic periodicities. *J. Hydrol.* 572, 226–242. doi: 10.1016/j.jhydrol.2019.02.060
- Lionello, P., and Scarascia, L. (2018). The relation between climate change in the Mediterranean region and global warming. *Reg. Environ. Chang.* 18, 1481–1493. doi: 10.1007/s10113-018-1290-1
- Lisar, S. Y. S., Motafakkerzad, R., Hossain, M. M., and Rahman, I. M. M. (2012). "Water stress in plants: causes, effects and responses" in Water Stress. eds. M. Rahman and H. Hasegawa (Rijeka, Croatia: In Tech), 1–14.
- Liu, J., Hu, D., Wang, H., Jiang, L., and Lu, G. (2022). Scale effects on the relationship between plant diversity and ecosystem multi functionality in arid desert areas. *Forests* 13:1505. doi: 10.3390/f13091505
- Longuevergne, L., Scanlon, B. R., and Wilson, C. R. (2010). GRACE hydrological estimates for small basins: Evaluating processing approaches on the High Plains Aquifer, USA. *Water Resour. Res.* 46. doi: 10.1029/2009WR008564
- Luthcke, S. B., Sabaka, T. J., Loomis, B. D., Arendt, A. A., McCarthy, J. J., and Camp, J. (2013). Antarctica, Greenland and Gulf of Alaska land-ice evolution from an iterated GRACE global mascon solution. *J. Glaciol.* 59, 613–631. doi: 10.3189/2013JG12J147
- Mahdaoui, K., Chafiq, T., Asmlal, L., and Tahiri, M. (2024). Assessing hydrological response to future climate change in the Bouregreg watershed, Morocco. *Sci. Afr.* 23:e02046. doi: 10.1016/j.sciaf.2023.e02046
- Mahe, G., Benabdelfadel, H., Dieulin, C., Elbaraka, M., Ezzaoui, M., Khomsi, K., et al. (2014). Evolution des débits liquides et solides du Bouregreg. In Gestion Durable des Terres. Proceedings de la Réunion Multi-Acteurs Sur le Bassin du Bouregreg. CERGeo, Faculté des Lettres et Sciences Humaines, Université Mohammed V-Agdal, Rabat, 28 mai 2013; Laouina, A., Mahe, G., Eds.; Edité par ARGDT: Rabat, Morocco; pp. 21–36.
- McKee, T. B., Doesken, N. J., and Kleist, J. (1993). The relationship of drought frequency and duration to time scales, p. 6.
- MEF (2015) Tableau de bord sectoriel. Ministère de l'Economie et des Finances, Royaume du Maroc, May 2015, p. 88. (Sectorial dashboard. Ministry of Economy and Finance, Kingdom of Morocco, May 2015, p. 88).
- Meliho, M., Khattabi, A., Jobbins, G., and Sghir, F. (2020). Impact of meteorological drought on agriculture in the Tensift watershed of Morocco. *J. Water Clim. Chang.* 11, 1323–1338. doi: 10.2166/wcc.2019.279
- Millennium Ecosystem Assessment (2005). Ecosystems and human well-being: Synthesis. Washington, DC: Island Press.
- Mishra, A. K., and Singh, V. P. (2010). A review of drought concepts. *J. Hydrol.* 391, 202–216. doi: 10.1016/j.jhydrol.2010.07.012
- Monteith, J. L. (1965). Evaporation and environment. In: 19th Symposia of the Society for Experimental Biology, University Press, Cambridge, pp. 205e234.
- NASA (2010). Science plan for NASA's science mission directorate, Tech. Rep., National Aeronautics and Space Administration, Washington, DC.
- Neves, M. C., Nunes, L. M., and Monteiro, J. P. (2020). Evaluation of GRACE data for water resource management in Iberia: a case study of groundwater storage monitoring in the Algarve region. *J. Hydrol. Reg. Stud.* 32:100734. doi: 10.1016/j.ejrh.2020.100734
- Nilsson, C., Reidy, C. A., Dynesius, M., and Revenga, C. (2005). Fragmentation and flow regulation of the world's large river systems. *Science* 308, 405–408. doi: 10.1126/science.1107887
- Ouassou, A., Ameziane, T., Ziyad, A., and Belghiti, M. (2005) Application of the drought management guidelines in Morocco. In MEDROPLAN Mediterranean drought preparedness and mitigation planning; Morocco; Chapter 19. Available at: https://projects.iamz.ciheam.org/medroplan/guidelines/archivos/Guidelines_Chapter19.pdf
- Quatiki, H., Boudhar, A., Leblanc, M., Fakir, Y., and Chehbouni, A. (2022). When climate variability partly compensates for groundwater depletion: an analysis of the GRACE signal in Morocco. *J. Hydrol. Reg. Stud.* 42:101177. doi: 10.1016/j.ejrh.2022.101177
- Quatiki, H., Boudhar, A., Ouhinou, A., Arioua, A., Hssaisoune, M., Bouamri, H., et al. (2019). Trend analysis of rainfall and drought over the Oum Er-Rbia River basin in Morocco during 1970–2010. *Arab. J. Geosci.* 12:128. doi: 10.1007/s12517-019-4300-9
- Ouhamdouch, S., Bahir, M., Ouazar, D., and Rafik, A. (2022). Hydrochemical characteristics of aquifers from the coastal zone of the Essaouira Basin (Morocco) and their suitability for domestic and agricultural uses. *Sustain. Water Resour. Manag.* 8, 1–15. doi: 10.1007/s40899-022-00754-6
- Ouharba, E. L., and Triqui, Z. E. L. (2022). Frequent And Extreme Climate Events In The BouregregWatershed (Morocco). *Neuro Quantology*, 20, 2418–2425. doi: 10.14704/nq.2022.20.9.NQ44283
- Ouharba, E. L., Mabrouki, J., and Triqui, Z. E. L. (2024). Assessment and future climate dynamics in the Bouregreg Basin, Morocco—impacts and adaptation alternatives. *Ecol. Eng. Environ. Technol.* 25, 51–63. doi: 10.12912/27197050/177823
- Pardo-Igúzquiza, E., Montillet, J.-P., Sánchez-Morales, J., Dowd, P. A., Luque-Espinar, J. A., Darbeheshti, N., et al. (2023). Assessing terrestrial water storage variations in southern Spain using rainfall estimates and grace data. *Hydrology* 10:187. doi: 10.3390/hydrology10090187

- Penman, H. L. (1948). Natural evaporation from open water, bare soil, and grass. *Proc. R. Soc. Lond. A* 193:116e140.
- Penning, E., Burgos, R. P., Mens, M., et al. (2023). Nature-based solutions for floods and droughts and biodiversity: do we have sufficient proof of their functioning? *Cambridge Prism Water* 1:e11. doi: 10.1017/wat.2023.12
- Pokhrel, Y., Felfelani, F., Satoh, Y., Boulange, J., Burek, P., Gädeke, A., et al. (2021). Global terrestrial water storage and drought severity under climate change. *Nat. Clim. Chang.* 11, 226–233. doi: 10.1038/s41558-020-00972-w
- Rafik, A., Ait Brahim, Y., Amazirh, A., Ouarani, M., Bargam, B., Ouatiqi, H., et al. (2023a). Groundwater level forecasting in a data-scarce region through remote sensing data downscaling, hydrological modeling, and machine learning: A case study from Morocco. *J. Hydrol. Reg. Stud.* 50:101569. doi: 10.1016/j.ejrh.2023.101569
- Rafik, A., Ait Brahim, Y., Ouahmouch, S., Bouchaou, L., Rhoujjati, N., and Chehbouni, A. (2023b). A multi-tool 3D conceptual model to elucidate groundwater processes, vulnerability, and recharge patterns in a semi-arid region: A case study from Morocco. *Earth Syst. Environ.* 7, 781–800. doi: 10.1007/s41748-023-00353-1
- Rasheed, M. W., Tang, J., Sarwar, A., Shah, S., Saddique, N., Khan, M. U., et al. (2022). Soil moisture measuring techniques and factors affecting the moisture dynamics: A comprehensive review. *Sustain. For.* 14:11538. doi: 10.3390/su141811538
- Rbaibi, O., and SahibEddine, A. (2024). “Sustainability in integrated water resources management: systematic literature review” in Technical and technological solutions towards a sustainable society and circular economy, World Sustainability Series. eds. J. Mabrouki and A. Mourade (Cham: Springer).
- Reyniers, N., Osborn, T. J., Addor, N., and Darch, G. (2023). Projected changes in droughts and extreme droughting in Great Britain strongly influenced by the choice of drought index. *Hydrol. Earth Syst. Sci.* 27, 1151–1171. doi: 10.5194/hess-27-1151-2023
- Rembold, F., Meroni, M., Urbano, F., Csak, G., Kerdiles, H., Perez-Hoyos, A., et al. (2019). ASAP: a new global early warning system to detect anomaly hot spots of agricultural production for food security analysis. *Agric. Syst.* 168, 247–257. doi: 10.1016/j.agsy.2018.07.002
- Rizwan, A. M., Dennis, L. Y. C., and Liu, C. (2008). A review on the generation, determination and mitigation of urban Heat Island. *J. Environ. Sci.* 20, 120–128. doi: 10.1016/S1001-0742(08)60019-4
- Rodell, M., and Famiglietti, J. S. (2001). An analysis of terrestrial water storage variations in Illinois with implications for the Gravity Recovery and Climate Experiment (GRACE). *Water Resour. Res.* 37, 1327–1339. doi: 10.1029/2000WR900306
- Rodell, M., Famiglietti, D. N., Wiese, J. T., Reager, H. K., Volaire, F., Beaudoin, F. W., et al. (2018). Merging trends in global freshwater availability. *Nature* 557, 651–659.
- Rome, S., Bigot, S., Chaffard, V., and Biron, P.-E. (2008). Relation entre les températures de l'air et les températures du sol: l'exemple des Hauts Plateaux du Vercors. Actes du colloque de l'Association Internationale de Climatologie, 21. Montpellier, Septembre 2008, 555–560.
- Saharwardi, M. S., Kumar, P., Dubey, A. K., and Kumari, A. (2022). Understanding spatiotemporal variability of drought in recent decades and its drivers over identified homogeneous regions of India. *Q. J. R. Meteorol. Soc.* 148, 2955–2972. doi: 10.1002/qj.4345
- Saher, R., Stephen, H., and Ahmad, S. (2021). Effect of land use change on summer time surface temperature, albedo, and evapotranspiration in Las Vegas Valley. *Urban Clim.* 39:100966. doi: 10.1016/j.uclim.2021.100966
- Samaniego, L., Thober, S., Kumar, R., Wanders, N., Rakovec, O., Pan, M., et al. (2018). Anthropogenic warming exacerbates European soil moisture droughts. *Nat. Clim. Chang.* 8, 421–426. doi: 10.1038/s41558-018-0138-5
- Saouabe, T., Ait Naceur, K., El Khalki, E. M., Hadri, A., and Saidi, M. E. (2022). GPM-IMERG product: a new way to assess the climate change impact on water resources in a Moroccan semi-arid basin. *Journal of Water and Climate Change* 13, 2559–2576. doi: 10.2166/wcc.2022.403
- Save, H., Bettadpur, S., and Tapley, B. D. (2016). High-resolution CSR GRACE RL05 mascons. *J. Geophys. Res. Solid Earth*, 121, 7547–7569. doi: 10.1002/2016JB013007
- Sarker, S. (2021). Investigating topologic and geometric properties of synthetic and Natural River networks under changing climatic. Ph.D. Thesis, University of Central Florida, Orlando, FL, USA. Available at: <https://stars.library.ucf.edu/etd2020/965>
- Sarker, S. (2022). Fundamentals of climatology for engineers: lecture note. *Eng* 3, 573–595. doi: 10.3390/eng3040040
- Schaaf, C. B. (2009). Albedo and reflectance anisotropy: Assessment of the status of the development of the standards for the terrestrial essential climate variables; Global Terrestrial Observing System: Rome, Italy.
- Schwarz, N., Schlink, U., Franck, U., and Großmann, K. (2012). Relationship of land surface and air temperatures and its implications for quantifying urban heat island indicators – an application for the city of Leipzig (Germany). *Ecol. Indic.* 18, 693–704. doi: 10.1016/j.ecolind.2012.01.001
- Shahid, S., and Hazarika, M. K. (2010). Groundwater drought in the northwestern districts of Bangladesh. *Water Resour. Manag.* 24, 1989–2006. doi: 10.1007/s11269-009-9534-y
- Shen, H., Leblanc, M., Tweed, S., and Liu, W. (2015). Groundwater depletion in the Hai River basin, China, from in situ and GRACE observations. *Hydrol. Sci. J.* 60, 671–687. doi: 10.1080/02626667.2014.916406
- Siebert, S., Kumm, M., Porkka, M., Döll, P., Ramankutty, N., and Scanlon, B. R. (2015). A global data set of the extent of irrigated land from 1900 to 2005. *Hydrol. Earth Syst. Sci.* 19, 1521–1545. doi: 10.5194/hess-19-1521-2015
- Singh, R. P., Roy, S., and Kogan, F. (2003). Vegetation and temperature condition indices from NOAA AVHRR data for drought monitoring over India. *Int. J. Remote Sens.* 24, 4393–4402. doi: 10.1080/0143116031000084323
- Singhal, A., Jaseem, M., Sarker, S., Prajapati, P., Singh, A., and Jha, S. K. (2023). Identifying potential locations of hydrologic monitoring stations based on topographical and hydrological information. *Water Resource Manage.* 38, 369–384. doi: 10.1007/s11269-023-03675-x
- Stour, L., and Agoumi, A. (2009). Climatic drought in Morocco in recent decades. *Hydroecol. Appl.* 16, 215–232. doi: 10.1051/hydro/2009003
- Sun, Y., Liu, S., Dong, Y., Dong, S., and Shi, F. (2020). Effects of multi-time scales drought on vegetation dynamics in Qaidam River basin, Qinghai-Tibet plateau from 1998 to 2015. *Appl. Clim.* 141, 117–131. doi: 10.1007/s00704-020-03194-4
- Sun, W., Wang, P., Zhang, S., Zhu, D., Liu, J., Chen, J., et al. (2008). Using the vegetation condition index for time series drought occurrence monitoring in the Guanzhong plain, PR China. *Int. J. Remote Sens.* 29, 5133–5144. doi: 10.1080/01431160802036557
- Svoboda, M., Hayes, M., and Wood, D. (2012). Standardized precipitation index user guide. Switzerland: World Meteorological Organization Geneva.
- Taha, H. (1997). Urban climates and heat islands: albedo, evapotranspiration, and anthropogenic heat. *Energy Buildings* 25, 99–103. doi: 10.1016/S0378-7788(96)00999-1
- Tapley, B. D., Watkins, M. M., Flechtner, F., Reigber, C., Bettadpur, S., Rodell, M., et al. (2019). Contributions of GRACE to understanding climate change. *Nature Climate Change*, 9, 358–369. doi: 10.1038/s41558-019-0456-2
- Tate, E. L., and Gustard, A. (2000). “Drought definition: A hydrological perspective” in Drought and drought mitigation in Europe. Advances in natural and technological hazards research, vol. 14. eds. J. V. Vogt and F. Somma (Dordrecht: Springer).
- Taylor, R. G., Koussis, A. D., and Tindimugaya, C. (2009). Groundwater and climate in Africa – a review. *Hydrol. Sci. J.* 54, 655–664. doi: 10.1623/hysj.54.4.655
- Templeton, N. P., Vivoni, E. R., Wang, Z. H., and Schreiner-McGraw, A. P. (2018). Quantifying water and energy fluxes over different urban land covers in Phoenix, Arizona. *J. Geophys. Res. Atmos.* 123, 2111–2128. doi: 10.1002/2017JD027845
- Tigkas, D., Vangelis, H., and Tsakiris, G. (2012). Drought and climatic change impact on streamflow in small watersheds. *Sci. Total Environ.* 440, 33–41. doi: 10.1016/j.scitotenv.2012.08.035
- Tra Bi, Z. A. (2013). Study the impact of anthropogenic activities and the climate variability on the vegetation and the social uses, by use of the technology and agricultural statistics, on the basin versant du Bouregreg (Morocco). Doctoral thesis, Félix Houphouët Boigny University, Ivory Coast, Abidjan. Available at: https://iahs.info/uploads/dms/15534.69-403-410-359-56-Tra-Bi-AISH_approvedCORR.pdf.
- Tramblay, Y., Koutroulis, A., Samaniego, L., Vicente-Serrano, S. M., Volaire, F., Boone, A., et al. (2020). Challenges for drought assessment in the Mediterranean region under future climate scenarios. *Earth Sci. Rev.* 210:103348. doi: 10.1016/j.earscirev.2020.103348
- Tsakiris, G., and Vangelis, H. (2004). Towards a drought watch system based on spatial SPI. *Water Resour. Manag.* 18, 1–12. doi: 10.1023/B:WARM.0000015410.47014.a4
- Tsakiris, G., and Vangelis, H. (2005). Establishing a drought index incorporating evapotranspiration. *European water*, 10, 3–11.
- UNWWAP (2009). The 3rd United Nations world water development report: Water in a changing world (WWDR-3) and facing the challenges. New York: UNWWAP.
- Van Rooy, M. P. (1965). A rainfall anomaly index independent of time and space. *Notas* 14, 43–48.
- Veldkamp, T. I. E., Wada, Y., Aerts, J. C. J. H., Döll, P., Gosling, S. N., Liu, J., et al. (2017). Water scarcity hotspots travel downstream due to human interventions in the 20th and 21st century. *Nat. Commun.* 8:15697. doi: 10.1038/ncomms15697
- Verner, D., Treguer, D., Redwood, J., Christensen, J., McDonnell, R., Elbert, C., et al. (2018). Climate variability, drought, and drought Management in Morocco's agricultural sector. Washington, DC: World Bank.
- Vicente-Serrano, S. M., Beguería, S., and López-Moreno, J. I. (2010). A multiscalar drought index sensitive to global warming: the standardized precipitation evapotranspiration index. *J. Clim.* 23, 1696–1718. doi: 10.1175/2009JCLI2909.1
- Vicente-Serrano, S. M., Peña-Angulo, D., Beguería, S., Domínguez-Castro, F., Tomás-Burguera, M., Noguera, I., et al. (2022). Global drought trends and future projections. *Philos. Trans. R. Soc. A* 380:20210285. doi: 10.1098/rsta.2021.0285
- Vicente-Serrano, S. M., Van der Schrier, G., Beguería, S., Azorin-Molina, C., and Lopez-Moreno, J.-I. (2015). Contribution of precipitation and reference evapotranspiration to drought indices under different climates. *J. Hydrol.* 526, 42–54. doi: 10.1016/j.jhydrol.2014.11.025

- Wang, T., Tu, X., Singh, V. P., Chen, X., and Lin, K. (2021). Global data assessment and analysis of drought characteristics based on CMIP6. *J. Hydrol.* 596:126091. doi: 10.1016/j.jhydrol.2021.126091
- Wang, F., Wang, Z. M., Yang, H. B., Zhao, Y., Li, Z. H., and Jia Peng, W. (2018). Capability of remotely sensed drought indices for representing the spatio-temporal variations of the meteorological droughts in the Yellow River Basin. *Remote Sens.* 10:1834. doi: 10.3390/rs10111834
- Wardlow, B., Anderson, M. C., and Verdin, J. (2012). Remote sensing of drought: Innovative monitoring approaches. Boca Raton, FL: CRC Press, 484.
- Watkins, M. M., Wiese, D. N., Yuan, D.-N., Boening, C., and Landerer, F. W. (2015). Improved methods for observing Earth's time variable mass distribution with GRACE using spherical cap mascons. *J. Geophys. Res. Solid Earth* 120, 2648–2671. doi: 10.1002/2014JB011547
- Wells, N., Steve, G., and Hayes, M. J. (2004). A self-calibrating palmer drought severity index. *J. Clim.* 17, 2335–2351. doi: 10.1175/1520-0442(2004)017<2335:ASPDISI>2.0.CO;2
- Wiese, D. N., Landerer, F. W., and Watkins, M. M. (2016). Quantifying and reducing leakage errors in the JPL RL05M GRACE mascon solution. *J. Water Resour. Res.*, 52, 7490–7502. doi: 10.1002/2016WR019344
- Wilhite, D. (2000). Drought as a natural Hazard: concepts and definitions. In Drought mitigation center faculty publications A global assessment, vol. 1, pp. 3–18). Available at: <https://digitalcommons.unl.edu/droughtfacpub/69>.
- Wuillez, M.-N. (2019). Literature review on climate change in Morocco: observations, projections and impacts. *Pap. De Rech.* 1–33.
- Wu, B., Ma, Z., Boken, V. K., Zeng, H., Shang, J., Igor, S., et al. (2022). Regional differences in the performance of drought mitigation measures in 12 major wheat-growing regions of the world. *Agric. Water Manag.* 273:107888. doi: 10.1016/j.agwat.2022.107888
- Xia, H., Chen, Y., and Quan, J. (2018). A simple method based on the thermal anomaly index to detect industrial heat sources. *Int. J. Appl. Earth Obs. Geoinf.* 73, 627–637. doi: 10.1016/j.jag.2018.08.003
- Xu, M., Wen, X., Wang, H., Zhang, W., Dai, X., Song, J., et al. (2014). Effects of climatic factors and ecosystem responses on the inter-annual variability of evapotranspiration in a coniferous plantation in subtropical China. *PLoS ONE*. 9:e85593. doi: 10.1371/journal.pone.0085593
- Yeh, P. J.-F., and Eltahir, E. A. B. (2005). Representation of water table dynamics in a land surface scheme. Part I: Model development. *J. Climate* 18, 1861–1880. doi: 10.1175/JCLI3330.1
- Yeh, P. J. F., and Famiglietti, J. S. (2009). Regional groundwater evapotranspiration in Illinois. *J. Hydrometeorol.* 10, 464–478. doi: 10.1175/2008JHM1018.1
- Yang, Z., Cai, Y., and Mitsch, W. J. (2015). Ecological and hydrological responses to changing environmental conditions in China's river basins. *Ecol. Eng.* 76, 1–6. doi: 10.1016/j.ecoleng.2014.12.007
- Yue, S., and Pilon, P. (2004). A comparison of the power of the t test, Mann-Kendall and bootstrap tests for trend detection/Une comparaison de la puissance des tests t de student, de Mann-Kendall et du bootstrap pour la détection de tendance. *Hydrol. Sci. J.* 49, 21–37. doi: 10.1623/hysj.49.1.21.53996
- Zaitchik, B. F., Rodell, M., and Reichle, R. H. (2008). Assimilation of GRACE terrestrial water storage data into a land surface model: results for the Mississippi River basin. *J. Hydrometeorol.* 9, 535–548. doi: 10.1175/2007JHM951.1
- Zhang, J., and Shang, Y. (2023). Nexus of dams, reservoirs, climate, and the environment: A systematic perspective. *Int. J. Environ. Sci. Technol.* 20, 12707–12716. doi: 10.1007/s13762-023-04765-4
- Zhang, H., Yin, G., and Zhang, L. (2022a). Evaluating the impact of different normalization strategies on the construction of drought condition indices. *Agric. For. Meteorol.* 323:109045. doi: 10.1016/j.agrformet.2022.109045
- Zhao, M., Velicogna, I., and Kimball, J. S. (2017a). Satellite observations of regional drought severity in the continental United States using GRACE-based terrestrial water storage changes. *J. Clim.* 30, 6297–6308. doi: 10.1175/JCLI-D-16-0458.1
- Zhou, T., Niu, A., Huang, Z., Ma, J., and Xu, S. (2020). Spatial relationship between natural wetlands changes and associated influencing factors in mainland China. *ISPRS Int. J. Geo Inf.* 9:179. doi: 10.3390/ijgi9030179
- Zhou, X., Wang, P., Tansey, K., Ghent, D., Zhang, S., Li, H., et al. (2019). Drought monitoring using the Sentinel-3-based multiyear vegetation temperature condition index in the Guanzhong plain, China. *IEEE J. Sel. Topics Appl. Earth Observ. Remote Sens.* 13, 129–142. doi: 10.1109/JSTARS.2019.2953955
- Zhu, N., Wang, J., Luo, D., Wang, X., Shen, C., Wu, N., et al. (2024). Unveiling evapotranspiration patterns and energy balance in a subalpine forest of the Qinghai-Tibet plateau: observations and analysis from an eddy covariance system. *J. For. Res.* 35, 1–14. doi: 10.1007/s11676-024-01708-8
- Zscheischler, J., Michalak, A. M., Schwalm, C., Mahecha, M. D., and Zeng, N. (2014). Impact of large-scale climate extremes on biospheric carbon fluxes: an intercomparison based on MsTMIP data. *Global Biogeochem. Cycles* 28, 585–600. doi: 10.1002/2014GB004826